arXiv:2511.21497v1 [stat.CO] 26 Nov 2025

Nested ensemble Kalman filter for static parameter inference in nonlinear state-space models

Andrew Golightly[1]*, Sarah E. Heaps[1], Chris Sherlock[2], Laura, E. Wadkin[3], Darren J. Wilkinson[1]

[1] Department of Mathematical Sciences, Durham University, UK
[2] School of Mathematical Sciences, Lancaster University, UK
[3] School of Mathematics, Statistics and Physics, Newcastle University, UK

Abstract

The ensemble Kalman filter (EnKF) is a popular technique for performing inference in state-space models (SSMs), particularly when the dynamic process is high-dimensional. Unlike reweighting methods such as sequential Monte Carlo (SMC, *i.e.* particle filters), the EnKF leverages either the linear Gaussian structure of the SSM or an approximation thereof, to maintain diversity of the sampled latent states (the so-called ensemble members) via shifting-based updates. Joint parameter and state inference using an EnKF is typically achieved by augmenting the state vector with the static parameter. In this case, it is assumed that both parameters and states follow a linear Gaussian state-space model, which may be unreasonable in practice. In this paper, we combine the reweighting and shifting methods by replacing the particle filter used in the SMC^2 algorithm of Chopin et al., with the ensemble Kalman filter. Hence, parameter particles are weighted according to the estimated observed-data likelihood from the latest observation computed by the EnKF, and particle diversity is maintained via a resample-move step that targets the marginal parameter posterior under the EnKF. Extensions to the resulting algorithm are proposed, such as the use of a delayed acceptance kernel in the rejuvenation step and incorporation of nonlinear observation models. We illustrate the resulting methodology via several applications.

Keywords: ensemble Kalman filter, particle filter, SMC^2, state-space models

1 Introduction

State-space models (SSMs, *e.g.* Harvey, 1990; Shumway and Stoffer, 2006; Särkkä, 2013) provide a flexible framework for modelling time-series data. An SSM typically involves two components: a model describing the temporal evolution of the latent system state and a model linking the state to observations. When these components involve linear functions of the latent process, the result is a tractable state-space model, often referred to as a dynamic linear model in the discrete-time context (DLM, see *e.g.* West and Harrison, 2006; Petris et al., 2009). In this case, the tractable observed-data likelihood and smoothing process can be efficiently calculated (conditional on parameters) using a Kalman filter (Kalman, 1960) and joint state and parameter inference can proceed in the Bayesian context via Markov chain Monte Carlo (*e.g.* Carter and Kohn, 1994; Frühwirth-Schnatter, 1994; Gamerman and Lopes, 2006). For nonlinear state-space models, inference may proceed via pseudo-marginal methods (Andrieu and Roberts, 2009) and, in particular, particle MCMC (Andrieu et al., 2010).

*andrew.golightly@durham.ac.uk

The focus of this paper is sequential Bayesian inference for the parameters and latent states in nonlinear state-space models. From a state filtering perspective, particle filters (*e.g.* Gordon et al., 1993; Doucet and Johansen, 2011; Jacob, 2015) can be used to recycle posterior samples from one time point to the next through a series of simple reweighting and resampling steps. State and parameter filtering is complicated by the exponential decrease over time in distinct parameter particles. This issue can be mitigated through the use of resample-move (also known as mutation) steps, which rejuvenate parameter particles via a Metropolis-Hastings kernel that has invariant distribution given by the parameter posterior. An example of the resulting scheme in the context of a tractable observed-data likelihood can be found in Chopin (2002). A pseudo-marginal analogue of this scheme, applicable in the intractable observed-data likelihood context, weights parameter particles by a likelihood estimate obtained from a particle filter over states, and rejuvenates parameter particles via a pseudo-marginal Metropolis-Hastings kernel. The resulting algorithm is termed SMC^2 (Chopin et al., 2013), due to the nested use of particle filters.

It is well known that particle filters suffer from weight degeneracy for high-dimensional targets (see Agapiou et al., 2017, for a discussion). Moreover, the simplest, bootstrap particle filter propagates particles myopically, irrespective of the next observation, which can lead to highly variable weights when observation noise is small relative to the noise in the state process. These problems are addressed, at the expense of some inferential accuracy, by the ensemble Kalman filter (EnKF, Evensen, 1994; see also Katzfuss et al., 2016 for an introduction), which has been ubiquitously applied in a field of research originating in the geosciences termed *data assimilation* (*e.g.* Evensen et al., 2022). As with the bootstrap particle filter, the EnKF propagates a set of simulations (known as ensemble members) via forward simulation of the state process. Unlike the reweighting of the particle filter, samples are shifted by a vector whose distribution depends on the next observation by leveraging a Gaussian approximation of the state distribution at the observation time, and if need be, of the observation model.

Compared to the state filtering problem, relatively few works have addressed both state and parameter filtering. Moreover, commonly used approaches are often based on strong assumptions. For example, *state augmentation* (*e.g.* Anderson, 2001; Evensen, 2009), assumes a linear Gaussian relationship between parameters, observations and states, with the latter augmented to include all parameter components. Several sequential and batch inference schemes are given in Katzfuss et al. (2019) (see also Stroud et al., 2018) in the context of dynamic parameters. These are applicable in the static parameter context through the assumption of an artificial evolution kernel, as has also been used in the particle filter context (*e.g.* Liu and West, 2001). However, this approach can be sensitive to the choice of tuning parameters (Vieira and Wilkinson, 2016).

Our contribution is a scheme for state and parameter filtering in which parameter particles are weighted by an approximate observed-data likelihood contribution, computed using the EnKF. Parameter rejuvenation mutates particles through a Metropolis-Hastings kernel that again uses the EnKF to calculate the likelihood for new parameter values. This corresponds to one iteration of the (offline) ensemble MCMC strategy of Katzfuss et al. (2019) and Drovandi et al. (2022). The resulting *nested ensemble Kalman filter (NEnKF)* uses the same nesting approach as SMC^2, albeit with the particle filter over states replaced by the EnKF. Given the robustness of the EnKF over a particle filter in high-dimensional settings, we anticipate that the NEnKF will be of most benefit to practitioners working with models in which the number of static parameter components is small relative to the dimension of the hidden state process. Several examples of such a scenario are given in Katzfuss et al. (2019).

As with SMC^2, the resample-move step in the NEnKF is the main computational bottleneck, and we therefore aim to improve its efficiency through the use of a delayed-acceptance kernel (e.g. Christen and Fox, 2005; Golightly et al., 2015; Banterle et al., 2019) that first tries proposals using a

simple k-nearest neighbour approximation to the observed data likelihood, that can be constructed dynamically using the current particle set. We also consider the case of nonlinear observation models, by using the EnKF to propagate the state process inside a particle filter. Unlike related approaches which use the EnKF as a proposal mechanism (e.g. Bi et al., 2015; Tamboli, 2021), our novel method allows for marginalising the latent state process between observation times.

The remainder of this paper is organised as follows. Section 2 introduces necessary background material on state-space models, the particle filter and SMC^2. Section 3 considers existing approaches to inference based on the EnKF. Section 4 outlines our proposed approach to the filtering problem and several extensions thereof. Applications of the proposed methodology are considered in Section 5 and conclusions drawn in Section 6.

2 Background

This section describes the relevant preliminary material. In particular, we consider state-space models and the inference objective in Section 2.1, the particle filter is detailed in Section 2.2 and its use inside SMC^2 is described in Section 2.3.

2.1 State-space models and inference task

A state-space model is defined for a fixed parameter vector $\theta = (\theta_1, \ldots, \theta_{d_\theta}) \in \Theta$ by the hidden / latent state dynamics $X_{0:t} := (X_0, \ldots, X_t)$, $X_t \in \mathsf{X}$, given by initial distribution $X_0 \sim p_0^{(\theta)}(\cdot)$, and

$$\begin{aligned} X_t &\sim p_t^{(\theta)}(\cdot|x_{t-1}), \qquad t = 1, \ldots, T, \\ Y_t &\sim f_t^{(\theta)}(\cdot|x_t), \qquad t = 0, \ldots, T. \end{aligned}$$

Here, $p_t^{(\theta)}(\cdot|x)$ and $f^{(\theta)}(\cdot|x)$ are conditional probability densities given x, and $Y_{0:T}$, $Y_t \in \mathsf{Y}$, is the resulting sequence of observations. Unless stated otherwise, we will assume that each X_t and Y_t are random vectors with support $\mathsf{X} = \mathbb{R}^{d_x}$ and $\mathsf{Y} = \mathbb{R}^{d_y}$ respectively.

The joint density of the hidden states and observations is given by

$$p_T^{(\theta)}(x_{0:T}, y_{0:T}) = \left\{ \prod_{t=0}^{T} f_t^{(\theta)}(y_t|x_t) \right\} p_0^{(\theta)}(x_0) \prod_{t=1}^{T} p_t^{(\theta)}(x_t|x_{t-1}).$$

Marginalising out the hidden states gives the *observed-data likelihood*

$$p_T^{(\theta)}(y_{0:T}) = p_0^{(\theta)}(y_0) \prod_{t=1}^{T} p_t^{(\theta)}(y_t|y_{0:t-1}).$$

From a Bayesian perspective, inference for the static parameters may proceed via the marginal parameter posterior

$$\pi_T(\theta|y_{0:T}) \propto \pi(\theta) p_T^{(\theta)}(y_{0:T}) \tag{1}$$

where $\pi(\theta)$ is the prior density ascribed to θ. If desired, samples of the hidden states can be generated from the smoothing density $p_T^{(\theta)}(x_{0:T}|y_{0:T})$, which is proportional to $p_T^{(\theta)}(x_{0:T}, y_{0:T})$.

In this article, the goal is sequential inference via recursive use of filtering densities of the form

$$\pi_t(\theta, x_t|y_{0:t}) = \pi_t(\theta|y_{0:t}) p_t^{(\theta)}(x_t|y_{0:t}), \quad t = 0, 1, \ldots, T. \tag{2}$$

For a fixed and known parameter θ, recursive exploration of the filtering densities over hidden states, $p_t^{(\theta)}(x_t|y_{0:t})$, $t = 0, 1, \ldots, T$, is typically achieved via a particle filter, which we consider in the next section.

2.2 Particle filter

The bootstrap particle filter (see *e.g.* Gordon et al., 1993) consists of a sequence of weighted resampling steps, whereby upon receipt of y_t, N state *particles* $x_{t-1}^{1:N} = \{x_{t-1}^1, \ldots, x_{t-1}^N\}$ are propagated forward via some proposal density, appropriately weighted and resampled with replacement.

The particle filter operates recursively as follows. The filtering density at time t can be written as

$$p_t^{(\theta)}(x_t|y_{0:t}) \propto f_t^{(\theta)}(y_t|x_t) \int p_t^{(\theta)}(x_t|x_{t-1}) p_{t-1}^{(\theta)}(x_{t-1}|y_{0:t-1}) dx_{t-1} \tag{3}$$

which is typically intractable. A weighted sample $\{x_{t-1}^{1:N}, w_{t-1}^{1:N}\}$ from $p_{t-1}^{(\theta)}(x_{t-1}|y_{0:t-1})$ admits the approximation

$$\widehat{p}_t^{(\theta)}(x_t|y_{0:t}) \propto f_t^{(\theta)}(y_t|x_t) \sum_{j=1}^{N} p_t^{(\theta)}(x_t|x_{t-1}^j) w_{t-1}^j,$$

which is sampled by first drawing an x_{t-1}^j with probability w_{t-1}^j then propagating according to a proposal density $q_t^{(\theta)}(x_t|x_{t-1}, y_t)$ and finally, reweighting accordingly. This weighted resampling scheme is presented in Algorithm 1, recursive application of which corresponds to the particle filter. Note that at time $t = 0$, steps 2–3 are implemented such that the propagate step draws $x_0^j \sim p_0^{(\theta)}(\cdot)$ and then the (unnormalised) weight is computed as $f_0^{(\theta)}(y_0|x_0^j)$.

Algorithm 1 Particle filter (step t)

Input: parameter θ and weighted particles $\{x_{t-1}^{1:N}, w_{t-1}^{1:N}\}$.

for $j = 1, 2, \ldots, N$ **do**

1. **Resample**. Sample an index a_{t-1}^j from $\{1, \ldots, N\}$ with probabilities $w_{t-1}^{1:N}$.
2. **Propagate**. Sample $x_t^j \sim q_t^{(\theta)}(\cdot|x_{t-1}^{a_{t-1}^j}, y_t)$.
3. **Weight**. Construct and normalise the weight

$$\tilde{w}_t(x_{t-1}^{a_{t-1}^j}, x_t^j) = \frac{p_t^{(\theta)}(x_t^j|x_{t-1}^{a_{t-1}^j}) f_t^{(\theta)}(y_t|x_t^j)}{q_t^{(\theta)}(x_t^j|x_{t-1}^{a_{t-1}^j}, y_t)}, \quad w_t^j = \tilde{w}_t(x_{t-1}^{a_{t-1}^j}, x_t^j) / \sum_{k=1}^{N} \tilde{w}_t(x_{t-1}^{a_{t-1}^k}, x_t^k).$$

end for

Output: likelihood estimate $\widehat{p}_t^{(\theta)}(y_t|y_{0:t-1}, x_t^{1:N}, a_{t-1}^{1:N}) = \frac{1}{N} \sum_{j=1}^{N} \tilde{w}_t(x_{t-1}^{a_{t-1}^j}, x_t^j)$ and weighted particles $\{x_t^{1:N}, w_t^{1:N}\}$.

The particle filter can be used to unbiasedly estimate the observed-data likelihood via the product (over time) of the average unnormalised weights (see *e.g.* Del Moral, 2004; Pitt et al., 2012). The estimator is

$$\begin{aligned} \widehat{p}_T^{(\theta)}(y_{0:T}|x_{0:T}^{1:N}, a_{0:T-1}^{1:N}) &= \widehat{p}_0^{(\theta)}(y_0|x_0^{1:N}) \times \prod_{t=1}^{T} \widehat{p}_t^{(\theta)}(y_t|y_{0:t-1}, x_t^{1:N}, a_{t-1}^{1:N}) \\ &= N^{-T-1} \sum_{j=1}^{N} \tilde{w}_0(x_0^j) \times \prod_{t=1}^{T} \left\{ \sum_{j=1}^{N} \tilde{w}_t(x_{t-1}^{a_{t-1}^j}, x_t^j) \right\} \end{aligned} \tag{4}$$

which we let depend explicitly on the particles $x_{0:T}^{1:N}$ and their genealogy $a_{0:T-1}^{1:N}$. In the context of batch inference for the static parameters θ, (4) can be used inside a pseudo-marginal Metropolis-Hastings (PMMH) scheme which exactly targets $\pi_T(\theta|y_{0:T})$ (see *e.g.* Andrieu et al., 2010). The contributions in (4) can also be used as incremental weights in a particle filter over static parameters, which we briefly review in the next section.

2.3 SMC^2

Suppose now that θ is unknown and interest lies in recursive learning of $\pi_t(\theta|y_{0:t})$, $t = 0, \ldots, T$. Sequential use of Bayes Theorem gives

$$\pi_t(\theta|y_{0:t}) \propto \pi_{t-1}(\theta|y_{0:t-1}) p_t^{(\theta)}(y_t|y_{0:t-1}) \tag{5}$$

which is complicated by the observed-data likelihood $p_t^{(\theta)}(y_t|y_{0:t-1})$, which is typically unavailable in closed form. Given a weighted sample of size M, $\{\theta^{1:M}, u_{t-1}^{1:M}\}$, from $\pi_{t-1}(\theta|y_{0:t-1})$, an idealised SMC scheme generates a weighted sample distributed according to (5) by reweighting each θ^i according to $u_t^i \propto u_{t-1}^i p_t^{(\theta^i)}(y_t|y_{0:t-1})$. Triggered by the fulfilment of some degeneracy criterion, such as that related to (6), below, a resample-move step (see *e.g.* Gilks and Berzuini, 2001) generates new parameter particles via a Metropolis-Hastings kernel that has (5) as its invariant distribution. Full details of the resulting iterated batch importance sampling (IBIS) scheme are given in Chopin (2002).

We consider here the pseudo-marginal analogue of IBIS (termed *SMC*^{2}, Chopin et al., 2013), wherein each θ^i particle is reweighted according to $u_t^i \propto u_{t-1}^i \widehat{p}_t^{(\theta^i)}(y_t|y_{0:t-1}, x_t^{i,1:N}, a_{t-1}^{i,1:N})$, and $\widehat{p}_t^{(\theta^i)}(y_t|y_{0:t-1}, x_t^{i,1:N}, a_{t-1}^{i,1:N})$ is the estimate of observed-data likelihood obtained by running Algorithm 1 with parameter θ^i and the associated state particle system $\{x_{t-1}^{i,1:N}, w_{t-1}^{i,1:N}\}$. Hence, over the entire observation period, each particle θ^i has associated state particles and genealogies $\{x_{0:T}^{i,1:N}, a_{0:T-1}^{i,1:N}\}$.

Parameter weight degeneracy is monitored via effective sample size (ESS), which is calculated at time t using the normalised parameter particle weights as

$$\text{ESS} = 1/\sum_{i=1}^{M} (u_t^i)^2. \tag{6}$$

If ESS falls below some user specified threshold, γM, a resample-move step is triggered by drawing M times from the mixture $\sum_{i=1}^{M} u_t^i K_t\left(\theta^i, \cdot\right)$, where K_t is a pseudo-marginal Metropolis-Hastings kernel with target $\pi_t(\theta|y_{0:t})$. Hence, after resampling, a new particle θ^* is proposed from a kernel $q(\theta^i, \cdot)$ and accepted with probability

$$\alpha(\theta^*|\theta^i) = 1 \wedge \frac{\pi(\theta^*)}{\pi(\theta^i)} \times \frac{\widehat{p}_t^{(\theta^*)}(y_{0:t}|x_{0:t}^{*,1:N}, a_{0:t-1}^{*,1:N})}{\widehat{p}_t^{(\theta^i)}(y_{0:t}|x_{0:t}^{i,1:N}, a_{0:t-1}^{i,1:N})} \times \frac{q(\theta^*, \theta^i)}{q(\theta^i, \theta^*)}. \tag{7}$$

A formal justification of SMC^2 can be found in Chopin et al. (2013); briefly, if $\psi_t^{(\theta)}(x_{0:t}^{1:N}, a_{0:t-1}^{1:N})$ denotes the joint probability density of all random variables generated by the state particle filter up to time t, then SMC^2 recursively targets

$$\widehat{\pi}_t(\theta, x_{0:t}^{1:N}, a_{0:t-1}^{1:N}|y_{0:t}) \propto \pi(\theta) \widehat{p}_t^{(\theta)}(y_{0:t}|x_{0:t}^{1:N}, a_{0:t-1}^{1:N}) \psi_t^{(\theta)}(x_{0:t}^{1:N}, a_{0:t-1}^{1:N})$$

which admits $\pi_t(\theta|y_{0:t})$ as a marginal.

Step t of SMC^2 is given in Algorithm 2 and assumes a fixed number of state particles, N. Since our goal is filtering via (2), we only store $\{\theta^i, u_t^i\}$ and the associated weighted particles $\{x_t^{i,1:N}, w_t^{i,1:N}\}$ at the most recent time, giving a storage cost of $\mathcal{O}(MN)$. Conditional on θ^i, a draw from $p^{(\theta^i)}(x_t|y_{0:t})$ can be obtained by generating an index $n(i)$ from $\{1, \ldots, N\}$ with probabilities $w_t^{i,1:N}$ and returning $x_t^{i,n(i)}$.

Note that the overall acceptance rate of the mutation step will depend, *inter alia*, on the variance of the likelihood approximation, which can be controlled by dynamically choosing the number of state

Algorithm 2 SMC^2 (step t)

Input: weighted parameter particles $\{\theta^i, u_{t-1}^i\}$, associated weighted particles $\{x_{t-1}^{i,1:N}, w_{t-1}^{i,1:N}\}$ and likelihood evaluations $\widehat{p}_{t-1}^{(\theta^i)}(y_{0:t-1}|x_{0:t-1}^{i,1:N}, a_{0:t-2}^{i,1:N})$, $i = 1, \ldots, M$.

for $i = 1, 2, \ldots, M$ **do**

1. Update weights and likelihood. Run Algorithm 1 with inputs θ^i and $\{x_{t-1}^{i,1:N}, w_{t-1}^{i,1:N}\}$ to obtain $\widehat{p}_t^{(\theta^i)}(y_t|y_{0:t-1}, x_t^{i,1:N}, a_{t-1}^{i,1:N})$ and $\{x_t^{i,1:N}, w_t^{i,1:N}\}$. Construct the weight

$$\tilde{u}_t^i = u_{t-1}^i \widehat{p}_t^{(\theta^i)}(y_t|y_{0:t-1}, x_t^{i,1:N}, a_{t-1}^{i,1:N})$$

and update the likelihood

$$\widehat{p}_t^{(\theta^i)}(y_{0:t}|x_{0:t}^{i,1:N}, a_{0:t-1}^{i,1:N}) = \widehat{p}_{t-1}^{(\theta^i)}(y_{0:t-1}|x_{0:t-1}^{i,1:N}, a_{0:t-2}^{i,1:N}) \widehat{p}_t^{(\theta^i)}(y_t|y_{0:t-1}, x_t^{i,1:N}, a_{t-1}^{i,1:N}).$$

if ESS $< \gamma M$ **then**

2. Resample. Normalise the weights to give $u_t^i = \tilde{u}_t^i / \sum_{k=1}^M \tilde{u}_t^k$. Sample an index b_i from $\{1, \ldots, M\}$ with probabilities $u_t^{1:M}$. Put $\{\theta^i, u_t^i\} := \{\theta_t^{b_i}, 1/M\}$ and $\{x_t^{i,1:N}, w_t^{i,1:N}\} := \{x_t^{b_i,1:N}, w_t^{b_i,1:N}\}$.

3. Move / mutate. Propose $\theta^* \sim q(\theta^i, \cdot)$. Perform iterations $1, \ldots, t$ of Algorithm 1 to obtain $\widehat{p}_t^{(\theta^*)}(y_{0:t}|x_{0:t}^{*,1:N}, a_{0:t-1}^{*,1:N})$ and $\{x_t^{*,1:N}, w_t^{*,1:N}\}$. With probability (7), put $\theta^i = \theta^*$, $\widehat{p}_t^{(\theta^i)}(y_{0:t}|x_{0:t}^{i,1:N}, a_{0:t-1}^{i,1:N}) = \widehat{p}_t^{(\theta^*)}(y_{0:t}|x_{0:t}^{*,1:N}, a_{0:t-1}^{*,1:N})$ and $\{x_t^{i,1:N}, w_t^{i,1:N}\} = \{x_t^{*,1:N}, w_t^{*,1:N}\}$.

end if

end for

Output: weighted parameter particles $\{\theta^i, u_t^i\}$, associated weighted particles $\{x_t^{i,1:N}, w_t^{i,1:N}\}$ and likelihood evaluations $\widehat{p}_t^{(\theta^i)}(y_{0:t}|x_{0:t}^{i,1:N}, a_{0:t-1}^{i,1:N})$, $i = 1, \ldots, M$.

particles N, for example, by doubling N if the empirical acceptance rate falls below some threshold chosen by the practitioner. For a given θ particle, state particles and their genealogies $\{x_{0:t}^{1:N}, a_{0:t-1}^{1:N}\}$ are replaced by $\{\check{x}_{0:t}^{1:\check{N}}, \check{a}_{0:t-1}^{1:\check{N}}\}$ (generated through recursive application of Algorithm 1) using the generalised importance sampling strategy of Del Moral et al. (2006). Implementation of this step implicitly weights each θ^i particle by

$$\frac{\widehat{\pi}_t(\theta^i, \check{x}_{0:t}^{i,1:\check{N}}, \check{a}_{0:t-1}^{i,1:\check{N}}|y_{0:t}) L_t^{(\theta^i)}\big(\{\check{x}_{0:t}^{i,1:\check{N}}, \check{a}_{0:t-1}^{i,1:\check{N}}\}, \{x_{0:t}^{1:N}, a_{0:t-1}^{i,1:N}\}\big)}{\widehat{\pi}_t(\theta^i, x_{0:t}^{i,1:N}, a_{0:t-1}^{i,1:N}|y_{0:t}) \psi_t^{(\theta)}(\check{x}_{0:t}^{i,1:\check{N}}, \check{a}_{0:t-1}^{i,1:\check{N}})}$$

where $L_t^{(\theta)}$ is an artificial backward kernel. As discussed in Chopin et al. (2013), although the optimal backward kernel is typically intractable, $L_t^{(\theta)}$ can be chosen to give a simple incremental weight of the form $\widehat{p}_t^{(\theta^i)}(y_{0:t}|\check{x}_{0:t}^{i,1:\check{N}}, \check{a}_{0:t-1}^{i,1:\check{N}}) / \widehat{p}_t^{(\theta^i)}(y_{0:t}|x_{0:t}^{i,1:N}, a_{0:t-1}^{i,1:N})$. On the other hand, Botha et al. (2023b) suggest a choice of backward kernel that introduces no additional variability in the particle weights; the incremental weight is 1 in this case.

3 Inference using the ensemble Kalman filter

In this section, we briefly review several existing methods for sequential state and parameter inference based on the ensemble Kalman filter (EnKF). For a detailed discussion, we refer the reader to Katzfuss et al. (2019).

3.1 Ensemble Kalman Filter

The ensemble Kalman filter (EnKF, see *e.g.* Evensen, 1994; Katzfuss et al., 2016) can be used to give approximate draws from the filtering densities $p_t^{(\theta)}(x_t|y_{0:t})$, $t = 0, 1, \ldots, T$. We assume here a linear and Gaussian observation model; extensions of the EnKF to other observation models are considered in Section 4.3.

Hence, consider

$$f_t^{(\theta)}(y_t|x_t) = \mathcal{N}(y_t; Hx_t, R) \tag{8}$$

where $\mathcal{N}(\cdot; \mu, \Sigma)$ denotes the density of a Gaussian random vector with mean μ and variance Σ. Additionally, H is a $d_y \times d_x$ matrix and R is a $d_y \times d_y$ variance matrix, and both of these may be functions of θ. The matrix H determines the observation regime; for example, taking $H = I$, the $d_x \times d_x$ identity matrix, gives a complete observation regime in which all elements of X_t are observed subject to Gaussian error. We assume throughout that H and R are constant, although the EnKF can accommodate time dependence of these quantities.

The EnKF operates recursively as follows. Suppose that a sample of size N *ensemble members* $x_{t-1}^{1:N} = \{x_{t-1}^1, \ldots, x_{t-1}^N\}$ is available at time $t-1$ from $p_{t-1}^{(\theta)}(x_{t-1}|y_{0:t-1})$. A forecast ensemble of size N is generated from $p_t^{(\theta)}(x_t|y_{0:t-1})$ by sampling $\tilde{x}_t^j \sim p_t^{(\theta)}(\cdot|x_{t-1}^j)$, $j = 1, \ldots, N$, to give $\tilde{x}_t^{1:N}$. Key to the operation of the EnKF is to approximate the forecast density as

$$\widehat{p}_{\text{enkf},t}^{(\theta)}(x_t|y_{0:t-1}, \tilde{x}_t^{1:N}) = \mathcal{N}(x_t\,;\, \hat{\mu}_{t|t-1}\,,\, \hat{\Sigma}_{t|t-1}) \tag{9}$$

where $\hat{\mu}_{t|t-1}$ and $\hat{\Sigma}_{t|t-1}$ are typically taken to be the sample mean and variance of the forecast ensemble $\tilde{x}_t^{1:N}$. Then, Bayes Theorem gives the approximation to the filtering density based on the EnKF as

$$\widehat{p}_{\text{enkf},t}^{(\theta)}(x_t|y_{0:t}, \tilde{x}_t^{1:N}) = \frac{\widehat{p}_{\text{enkf},t}^{(\theta)}(x_t|y_{0:t-1}, \tilde{x}_t^{1:N}) f_t^{(\theta)}(y_t|x_t)}{\widehat{p}_{\text{enkf},t}^{(\theta)}(y_t|y_{0:t-1}, \tilde{x}_t^{1:N})} \tag{10}$$

for which, under the linear Gaussian structure of (8) and (9), we obtain

$$\widehat{p}_{\text{enkf},t}^{(\theta)}(x_t|y_{0:t}, \tilde{x}_t^{1:N}) = \mathcal{N}(x_t\,;\, \hat{\mu}_{t|t}\,,\, \hat{\Sigma}_{t|t}) \tag{11}$$

where $\hat{\mu}_{t|t} = \hat{\mu}_{t|t-1} + \hat{K}_t(y_t - H\hat{\mu}_{t|t-1})$, $\hat{\Sigma}_{t|t} = (I - \hat{K}_t H)\hat{\Sigma}_{t|t-1}$ and $\hat{K}_t$ is an estimate of the Kalman gain, that is

$$\hat{K}_t = \hat{\Sigma}_{t|t-1} H'(H\hat{\Sigma}_{t|t-1}H' + R)^{-1}. \tag{12}$$

Although (11) can be sampled from trivially, it is common to perform a stochastic update step (see e.g. Katzfuss et al., 2016), which moves ensemble members according to a Gaussian pseudo-observation $\tilde{y}_t^j \sim \mathcal{N}(H\tilde{x}_t^j, R)$. New ensemble members are obtained as $x_t^j = \tilde{x}_t^j + \hat{K}_t(y_t - \tilde{y}_t^j)$ which avoids draws of dimension d_x (with $d_x >> d_y$ in common applications). Note that marginalising over x_t in (8) with respect to (9) gives the denominator in (10) (that is, observed data likelihood contribution) as

$$\widehat{p}_{\text{enkf},t}^{(\theta)}(y_t|y_{0:t-1}, \tilde{x}_t^{1:N}) = \mathcal{N}(y_t\,;\, H\hat{\mu}_{t|t-1}\,,\, H\hat{\Sigma}_{t|t-1}H' + R). \tag{13}$$

Algorithm 3 gives a summary of the above steps upon receipt of an observation y_t. The EnKF can be initialised at time $t = 0$ by sampling N ensemble members $\tilde{x}_0^{1:N}$ from $p_0^{(\theta)}(\cdot)$ and setting $\hat{\mu}_0$ and $\hat{\Sigma}_0$ to be the sample mean and variance of $\tilde{x}_0^{1:N}$. Equations (11)–(13) are applied with $\hat{\mu}_0$ and $\hat{\Sigma}_0$ replacing $\hat{\mu}_{t|t-1}$ and $\hat{\Sigma}_{t|t-1}$

Up until now, our discussion of the EnKF has assumed that the parameter θ is fixed and known. In the following three sections, we briefly review some existing methods for dealing with an unknown θ.

Algorithm 3 Ensemble Kalman filter (step t)

Input: parameter θ, ensemble members $x_{t-1}^{1:N}$.
for $j = 1, 2, \ldots, N$ **do**
1. Forecast ensemble. Sample $\tilde{x}_t^j \sim p_t^{(\theta)}(\cdot|x_{t-1}^j)$.
2. Update step. Set $x_t^j = \tilde{x}_t^j + \hat{K}_t(y_t - \tilde{y}_t^j)$, where $\tilde{y}_t^j \sim \mathcal{N}(H\tilde{x}_t^j, R)$ is a pseudo-observation.
end for
Output: likelihood increment $\widehat{p}_{\text{enkf},t}^{(\theta)}(y_t|y_{0:t-1}, \tilde{x}_t^{1:N}) = \mathcal{N}(y_t\,;\, H\hat{\mu}_{t|t-1}\,,\, H\hat{\Sigma}_{t|t-1}H' + R)$ and ensemble members $x_t^{1:N}$.

3.2 Ensemble MCMC

Recall the marginal parameter posterior $\pi_T(\theta|y_{0:T})$ given by (1). This can be approximated using the EnKF by considering the joint density

$$\begin{aligned}\widehat{\pi}_{\text{enkf},T}(\theta, \tilde{x}_{0:T}^{1:N}, x_{0:T}^{1:N}|y_{0:T}) &\propto \pi(\theta)\widehat{p}_{\text{enkf},T}^{(\theta)}(y_{0:T}|\tilde{x}_{0:T}^{1:N})\psi_T^{(\theta)}(\tilde{x}_{0:T}^{1:N}, x_{0:T}^{1:N}) \\ &\propto \pi(\theta)\left\{\widehat{p}_{\text{enkf},0}^{(\theta)}(y_0|\tilde{x}_0^{1:N})\prod_{t=1}^{T}\widehat{p}_{\text{enkf},t}^{(\theta)}(y_t|y_{0:t-1}, \tilde{x}_t^{1:N})\right\}\psi_T^{(\theta)}(\tilde{x}_{0:T}^{1:N}, x_{0:T}^{1:N}) \quad (14)\end{aligned}$$

where $\psi_T^{(\theta)}(\tilde{x}_{0:T}^{1:N}, x_{0:T}^{1:N})$ denotes the joint density of the entire ensemble $\{\tilde{x}_{0:T}^{1:N}, x_{0:T}^{1:N}\}$. Although (14) is typically intractable, it can be sampled using MCMC, and the parameter samples retained to give (dependent) draws from $\widehat{\pi}_{\text{enkf},T}(\theta|y_{0:T})$, the θ-marginal of (14). The resulting approach, termed *ensemble MCMC* (eMCMC) is detailed in Drovandi et al. (2022) (see also Stroud et al., 2018; Katzfuss et al., 2019). In brief, at iteration k, a new θ^* is proposed from a kernel $q(\theta^{k-1}, \cdot)$. Then, sampling of the corresponding ensemble $\{\tilde{x}_{0:T}^{*,1:N}, x_{0:T}^{*,1:N}\}$ from $\psi_T^{(\theta^*)}(\cdot, \cdot)$ and evaluation of the observed data likelihood $\widehat{p}_{\text{enkf},T}^{(\theta^*)}(y_{0:T}|\tilde{x}_{0:T}^{*,1:N})$, is achieved through recursive application of Algorithm 3. The parameter θ^* is retained with probability

$$\alpha_{\text{enkf}}(\theta^*|\theta^{k-1}) = 1 \wedge \frac{\pi(\theta^*)}{\pi(\theta^{k-1})} \times \frac{\widehat{p}_{\text{enkf},T}^{(\theta^*)}(y_{0:T}|\tilde{x}_{0:T}^{*,1:N})}{\widehat{p}_{\text{enkf},T}^{(\theta^{k-1})}(y_{0:T}|\tilde{x}_{0:T}^{k-1,1:N})} \times \frac{q(\theta^*, \theta^{k-1})}{q(\theta^{k-1}, \theta^*)}. \quad (15)$$

When applied sequentially, eMCMC is wasteful in terms of both storage and computational costs; upon receipt of a new observation (say y_{T+1}), previous parameter samples are discarded and eMCMC is run from scratch. Nevertheless, we use eMCMC for benchmarking the accuracy of various sequential approaches in the context of static parameter inference, for example, when running PMMH would be computationally prohibitive. It is also a key component of the resample-move step described in Section 4.

3.3 State augmentation

The EnKF can be directly modified to simultaneously estimate both hidden states and static parameters by augmenting the state vector x_t to incorporate θ (see e.g. Evensen, 2009; Mitchell and Arnold, 2021). We write $z_t = (x_t', \theta_t')'$ with x_t evolving according to $p_t^{(\theta)}(\cdot|x_{t-1})$ and $\theta_t = \theta_{t-1} = \theta$. The observation model becomes $f_t^{(\theta)}(y_t|z_t) = \mathcal{N}(y_t; H_z z_t, R)$ with $H_z = (H, 0_{d_y \times d_\theta})$, where $0_{d_y \times d_\theta}$ is a $d_y \times d_\theta$ matrix of zeros and H is not a function of θ.

The resulting augmented EnKF (AEnKF) operates recursively as follows. Suppose that a sample of size N ensemble members $\{x_{t-1}^{1:N}, \theta^{1:N}\}$ is available at time $t-1$ from the filtering distribution at time $t-1$. A forecast ensemble of size N is generated via $\tilde{x}_t^j \sim p_t^{(\theta)}(\cdot|x_{t-1}^j)$, $\tilde{\theta}_t = \theta_{t-1}$ and

setting $\tilde{z}_t^j = (\tilde{x}_t^{j\prime}, \tilde{\theta}_t^{j\prime})'$, $j = 1, \ldots, N$. The update step is given by $z_t^j = \tilde{z}_t^j + \hat{K}_{z,t}(y_t - \tilde{y}_t^j)$ where $\tilde{y}_t^j \sim \mathcal{N}(H_z \tilde{z}_t^j, R)$ is a pseudo-observation and the Kalman gain becomes

$$\hat{K}_{z,t} = \hat{\Sigma}_{t|t-1} H_z' (H_z \hat{\Sigma}_{t|t-1} H_z' + R)^{-1}. \tag{16}$$

where $\hat{\Sigma}_{t|t-1}$ is the sample covariance of the forecast ensemble $\tilde{z}_t^1, \ldots, \tilde{z}_t^N$.

To alleviate under-dispersion in the parameter ensemble, for example when small ensemble sizes are considered (*e.g.* Ruckstuhl and Janjić, 2018), the parameter vector can be allowed to dynamically evolve, for example using the artificial evolution kernel of Liu and West (2001), which gives

$$p_t(\theta_t|\theta_{t-1}) = \mathcal{N}\left(\theta_t; a\theta_{t-1} + (1-a)\bar{\theta}_{t-1}, h^2 V_{t-1}\right) \tag{17}$$

where $\bar{\theta}_{t-1}$ and V_{t-1} are the sample mean and variance of $\theta_{t-1}^1, \ldots, \theta_{t-1}^N$. Setting $a = \sqrt{1-h^2}$ corrects for over-dispersion; the practitioner can then choose the smoothing parameter h, for example using the discounting method of Liu and West (2001). Step t of the augmented EnKF is summarised by Algorithm 4.

Algorithm 4 Augmented ensemble Kalman filter (step t)

Input: ensemble members $\{x_{t-1}^{1:N}, \theta_{t-1}^{1:N}\}$.
for $j = 1, 2, \ldots, N$ **do**
1. Forecast ensemble. Sample $\tilde{\theta}_t^j \sim \mathcal{N}\left(a\theta_{t-1}^j + (1-a)\bar{\theta}_{t-1}, h^2 V_{t-1}\right)$ and $\tilde{x}_t^j \sim p_t^{(\tilde{\theta}_t^j)}(\cdot|x_{t-1}^j)$.
Set $\tilde{z}_t^j = (\tilde{x}_t^{j\prime}, \tilde{\theta}_t^{j\prime})'$.
2. Update step. Set $z_t^j = \tilde{z}_t^j + \hat{K}_{z,t}(y_t - \tilde{y}_t^j)$, where $\tilde{y}_t^j \sim \mathcal{N}(H_z \tilde{z}_t^j, R)$ is a pseudo-observation.
end for
Output: ensemble members $\{x_t^{1:N}, \theta_t^{1:N}\}$.

3.4 Particle ensemble Kalman filter (PEnKF)

The augmented EnKF makes the strong assumption that the parameters and observations follow a linear Gaussian structure. An alternative approach for dealing with the static parameters is to marginalise out the hidden states in a sequential fashion. Recall the factorisation of $\pi_t(\theta|y_{0:t})$ in (5) and the assumption of a weighted sample of size M, $\{\theta^{1:M}, u_{t-1}^{1:M}\}$, from $\pi_{t-1}(\theta|y_{0:t-1})$. Upon receipt of y_t, and in the context of time-varying parameters, Katzfuss et al. (2019) (see also Frei and Künsch, 2011, among others) propose to use the observed-data likelihood under the EnKF to reweight parameter particles. We adapt the resulting particle ensemble Kalman filter (PEnKF) to our problem as follows.

We impose the artificial evolution kernel (17) and consider a particle filter for recursive exploration of the target

$$\begin{aligned}
&\widehat{\pi}_{\text{enkf},t}(\theta_{0:t}, \tilde{x}_{0:t}^{1:N}, x_{0:t}^{1:N}|y_{0:t}) \\
&\propto \pi(\theta_0)\widehat{p}_{\text{enkf},0}^{(\theta_0)}(y_0|\tilde{x}_0^{1:N}) \left\{\prod_{s=1}^{t} \widehat{p}_{\text{enkf},s}^{(\theta_s)}(y_s|y_{0:s-1}, \tilde{x}_s^{1:N}) p_s(\theta_s|\theta_{s-1})\right\} \psi_t^{(\theta_{0:t})}(\tilde{x}_{0:t}^{1:N}, x_{0:t}^{1:N}) \\
&\propto \widehat{\pi}_{\text{enkf},t-1}(\theta_{0:t-1}, \tilde{x}_{0:t-1}^{1:N}, x_{0:t-1}^{1:N}|y_{0:t-1}) \widehat{p}_{\text{enkf},t}^{(\theta_t)}(y_t|y_{0:t-1}, \tilde{x}_t^{1:N}) p_t(\theta_t|\theta_{t-1}) \psi_t^{(\theta_t)}(\tilde{x}_t^{1:N}, x_t^{1:N}|x_{t-1}^{1:N})
\end{aligned}$$

where $\psi_t^{(\theta_t)}(\tilde{x}_t^{1:N}, x_t^{1:N}|x_{t-1}^{1:N})$ is the joint density of the ensemble $\{\tilde{x}_t^{1:N}, x_t^{1:N}\}$ (conditional on θ_t and $x_{t-1}^{1:N}$) and can be sampled via application of Algorithm 3 with inputs θ_t and $x_{t-1}^{1:N}$. From a filtering perspective, marginalising $\widehat{\pi}_{\text{enkf},t-1}$ over $\theta_{0:t-2}$, $x_{0:t-2}^{1:N}$ and $\tilde{x}_{0:t-1}^{1:N}$ gives a particle filter that only requires storage of the weighted parameter particles $\{\theta_{t-1}^i, u_{t-1}^i\}$ (representing a weighted sample

from the marginalised $\widehat{\pi}_{\text{enkf},t-1}$) and the associated ensemble members $x_{t-1}^{i,1:N}$, for $i = 1, \ldots, M$, at time $t-1$. As with our implementation of SMC^2 in Section 2.3, the storage cost of implementing PEnKF is then $\mathcal{O}(MN)$.

The PEnKF assimilates the information in y_t by first sampling $\theta_t^i \sim p_t(\cdot|\theta_{t-1}^i)$. The corresponding ensemble, $\{\tilde{x}_t^{i,1:N}, x_t^{i,1:N}\}$, is drawn from $\psi_t^{(\theta_t^i)}(\cdot, \cdot|x_{t-1}^{i,1:N})$ by running Algorithm 3 with parameter θ_t^i and ensemble members $x_{t-1}^{i,1:N}$. Finally, a new weight is constructed according to $u_t^i \propto u_{t-1}^i \widehat{p}_{\text{enkf},t}^{(\theta_t^i)}(y_t|y_{0:t-1}, \tilde{x}_t^{i,1:N})$.

Step t of the PEnKF is summarised by Algorithm 5. Note that we include a resampling step, which is triggered if the effective sample size (ESS) falls below some user specified threshold, γM . The ESS is calculated at time t using (6).

Algorithm 5 Particle ensemble Kalman filter (step t)

Input: weighted parameter particles $\{\theta_{t-1}^i, u_{t-1}^i\}$ and associated ensemble members $x_{t-1}^{i,1:N}$, $i = 1, \ldots, M$.
for $i = 1, 2, \ldots, M$ **do**
1. Update parameters. Sample $\theta_t^i \sim \mathcal{N}\left(a\theta_{t-1}^i + (1-a)\bar{\theta}_{t-1}, h^2 V_{t-1}\right)$.
2. Update weights. Run Algorithm 3 with inputs θ_t^i and $x_{t-1}^{i,1:N}$ to obtain $\widehat{p}_{\text{enkf},t}^{(\theta_t^i)}(y_t|y_{0:t-1}, \tilde{x}_t^{i,1:N})$ and $x_t^{i,1:N}$. Construct the weight

$$\tilde{u}_t^i = u_{t-1}^i \widehat{p}_{\text{enkf},t}^{(\theta_t^i)}(y_t|y_{0:t-1}, \tilde{x}_t^{i,1:N}).$$

if ESS $< \gamma M$ **then**
3. Resample. Normalise the weights to give $u_t^i = \tilde{u}_t^i / \sum_{k=1}^M \tilde{u}_t^k$. Sample an index b_i from $\{1, \ldots, M\}$ with probabilities $u_t^{1:M}$. Put $\{\theta_t^i, u_t^i\} := \{\theta_t^{b_i}, 1/M\}$ and $x_t^{i,1:N} := x_t^{b_i,1:N}$.
end if
end for
Output: weighted parameter particles $\{\theta_t^i, u_t^i\}$ and associated ensemble members $x_t^{i,1:N}$, $i = 1, \ldots, M$.

4 Nested ensemble Kalman filter (NEnKF)

From the perspective of static parameter filtering, the EnKF-based methods described in Section 3 attempt to mitigate particle degeneracy via an artificial evolution kernel over the static parameters. This can be sensitive to the choice of tuning parameters (Vieira and Wilkinson, 2016). The SMC^2 algorithm described in Section 2 provides a more principled approach to alleviating particle degeneracy: if triggered at some time t, a resample-move step mutates parameter particles through a (pseudo-marginal) Metropolis-Hastings kernel that has $\pi_t(\theta|y_{0:t})$ as its invariant distribution. However, both the weighting and resample-move step in SMC^2 require running a particle filter over states, which can require a computationally prohibitive number of state particles N in high-dimensional settings. For a specific example with $d_x = d_y =: n$, Katzfuss et al. (2019) show that the variance of the logarithm of observed-data likelihood under the EnKF, $\text{Var}[\log \widehat{p}_{\text{enkf},T}^{(\theta)}(y_{0:T}|\tilde{x}_{0:T}^{1:N})]$, can be controlled by scaling N linearly with n, whereas N should be scaled exponentially with n when controlling $\text{Var}[\log \widehat{p}_T^{(\theta)}(y_{0:T}|x_{0:T}^{1:N}, a_{0:T-1}^{1:N})]$, computed using a particle filter. When comparing the efficiency of ensemble MCMC and particle MCMC across several examples, Drovandi et al. (2022) find that the former can tolerate a much smaller value of N compared to the latter.

Our proposed approach leverages the robustness of the EnKF and the principled framework of SMC^2

by weighting static parameter particles by the EnKF likelihood and, where necessary, mutating these particles using the ensemble MCMC scheme described in Section 3.1. By analogy with SMC^2, we term the resulting algorithm *nested EnKF (NEnKF)*. In what follows, we provide the basic NEnKF algorithm before considering some extensions for improving efficiency.

4.1 NEnKF algorithm

The NEnKF recursively targets $\widehat{\pi}_{\text{enkf},t}(\theta, x_t^{1:N}|y_{0:t})$ which can be constructed by taking the extended target

$$\begin{aligned}\widehat{\pi}_{\text{enkf},t}(\theta, \tilde{x}_{0:t}^{1:N}, x_{0:t}^{1:N}|y_{0:t}) &\propto \pi(\theta)\widehat{p}_{\text{enkf},t}^{(\theta)}(y_{0:t}|\tilde{x}_{0:t}^{1:N})\psi_t^{(\theta)}(\tilde{x}_{0:t}^{1:N}, x_{0:t}^{1:N}) \\ &\propto \widehat{\pi}_{\text{enkf},t-1}(\theta, \tilde{x}_{0:t-1}^{1:N}, x_{0:t-1}^{1:N}|y_{0:t-1})\widehat{p}_{\text{enkf},t}^{(\theta)}(y_t|y_{0:t-1}, \tilde{x}_t^{1:N}) \\ &\quad \times \psi_t^{(\theta)}(\tilde{x}_t^{1:N}, x_t^{1:N}|x_{t-1}^{1:N})\end{aligned}$$

and marginalising out $\tilde{x}_{0:t}^{1:N}$ and $x_{0:t-1}^{1:N}$. Hence, given a weighted parameter sample $\{\theta^i, u_{t-1}^i\}$ with associated ensemble $x_{t-1}^{i,1:N}$, $i = 1, \ldots, M$, from $\widehat{\pi}_{\text{enkf},t-1}(\theta, x_{t-1}^{1:N}|y_{0:t-1})$, it should be clear that the weights are updated according to $u_t^i \propto u_{t-1}^i \widehat{p}_{\text{enkf},t}^{(\theta^i)}(y_t|y_{0:t-1}, \tilde{x}_t^{i,1:N})$, by running Algorithm 3 with parameter θ^i and ensemble members $x_{t-1}^{i,1:N}$.

Analagously to SMC^2, particle degeneracy is mitigated via a resample-move step. That is, when ESS (6) falls below a pre-specified threshold, γM, we draw M times from the mixture $\sum_{i=1}^M u_t^i K_{\text{enkf},t}\left(\theta^i, \cdot\right)$, where $\tilde{K}_t$ is an eMCMC kernel (see Section 3.2) with target $\pi_{\text{enkf},t}(\theta|y_{0:t})$. Hence, after resampling, with θ^i denoting the ith resampled particle, a new particle θ^* is proposed from a kernel $q(\theta^i, \cdot)$ and accepted with probability

$$\alpha_{\text{enkf}}(\theta^*|\theta^i) = 1 \wedge \frac{\pi(\theta^*)}{\pi(\theta^i)} \times \frac{\widehat{p}_{\text{enkf},t}^{(\theta^*)}(y_{0:t}|\tilde{x}_{0:t}^{*,1:N})}{\widehat{p}_{\text{enkf},t}^{(\theta^i)}(y_{0:t}|\tilde{x}_{0:t}^{i,1:N})} \times \frac{q(\theta^*, \theta^i)}{q(\theta^i, \theta^*)}. \tag{18}$$

Note that $\tilde{x}_{0:t}^{*,1:N}$ is implicitly generated by running the EnKF forward from time 0. In what follows, we take $q(\theta^i, \cdot)$ to be the kernel associated with a random walk Metropolis move of the form

$$\theta^* = \theta^i + \epsilon^i, \qquad \epsilon^i \sim \mathcal{N}(0, \zeta V_t).$$

To ensure a reversible move, the variance V_t can be computed as the sample variance of all resampled particles except the ith. The scaling ζ can be chosen by the practitioner or set using a rule of thumb, for example, in the pseudo-marginal context, Sherlock et al. (2015) suggest $\zeta^2 = 2.56^2/d_\theta$. Efficiency of the move step can be increased, at increased computational cost, by repeatedly sampling from $K_{\text{enkf},t}\left(\theta^i, \cdot\right)$. Although we do not pursue it here, adapting the number of MCMC iterations in the mutation step is discussed in the SMC^2 context in Botha et al. (2023b). Step t of the NEnKF can be found in Algorithm 6. Note that for ease of exposition, we present the algorithm for a fixed value N and for a single iteration of eMCMC (per parameter particle) in the mutation step.

Following the approach used in SMC^2, we also consider a mechanism for dynamically updating the number of ensemble members N. After completion of the mutation step, if updating N is triggered then for each particle θ^i, ensemble members $x_{0:t}^{i,1:N}$ are replaced by $\check{x}_{0:t}^{i,1:\check{N}}$ using the generalised importance sampling strategy of Del Moral et al. (2006), with an artificial backward kernel chosen to give an incremental weight of 1 (Botha et al., 2023b). Hence, for each particle θ^i, a new ensemble $\check{x}_{0:t}^{i,1:\check{N}}$ is generated through repeated application of Algorithm 3. Once the updating of N is triggered, we adapt the method of Duan and Fulop (2015) to our context, by setting $\check{N} = \hat{\sigma}_N^2 N$, where $\hat{\sigma}_N^2$ is an estimate of the variance of $\widehat{p}_{\text{enkf},t}^{(\bar{\theta})}(y_{0:t}|\tilde{x}_{0:t}^{1:N})$, based on, say, r runs of the EnKF

Algorithm 6 Nested ensemble Kalman filter (step t)

Input: weighted parameter particles $\{\theta^i, u_{t-1}^i\}$, associated ensemble members $x_{t-1}^{i,1:N}$ and likelihood evaluations $\widehat{p}_{\text{enkf},t-1}^{(\theta^i)}(y_{0:t-1}|\tilde{x}_{0:t-1}^{i,1:N})$, $i = 1, \ldots, M$.

for $i = 1, 2, \ldots, M$ **do**

1. Update weights and likelihood. Run Algorithm 3 with inputs θ^i and $x_{t-1}^{i,1:N}$ to obtain $\widehat{p}_{\text{enkf},t}^{(\theta^i)}(y_t|y_{0:t-1}, \tilde{x}_t^{i,1:N})$ and $x_t^{i,1:N}$. Construct the weight

$$\tilde{u}_t^i = u_{t-1}^i \widehat{p}_{\text{enkf},t}^{(\theta^i)}(y_t|y_{0:t-1}, \tilde{x}_t^{i,1:N})$$

and update the likelihood

$$\widehat{p}_{\text{enkf},t}^{(\theta^i)}(y_{0:t}|\tilde{x}_{0:t}^{i,1:N}) = \widehat{p}_{\text{enkf},t-1}^{(\theta^i)}(y_{0:t-1}|\tilde{x}_{0:t-1}^{i,1:N}) \widehat{p}_{\text{enkf},t}^{(\theta^i)}(y_t|y_{0:t-1}, \tilde{x}_t^{i,1:N}).$$

if ESS $< \gamma M$ **then**

2. Resample. Normalise the weights to give $u_t^i = \tilde{u}_t^i / \sum_{k=1}^M \tilde{u}_t^k$. Sample an index b_i from $\{1, \ldots, M\}$ with probabilities $u_t^{1:M}$. Put $\{\theta^i, u_t^i\} := \{\theta_t^{b_i}, 1/M\}$ and $x_t^{i,1:N} := x_t^{b_i,1:N}$.

3. Move / mutate. Propose $\theta^* \sim q(\theta^i, \cdot)$. Perform iterations $1, \ldots, t$ of Algorithm 3 to obtain $\widehat{p}_{\text{enkf},t}^{(\theta^*)}(y_{0:t}|\tilde{x}_{0:t}^{*,1:N})$ and $x_t^{*,1:N}$. With probability (18), put $\theta^i = \theta^*$, $\widehat{p}_{\text{enkf},t}^{(\theta^i)}(y_{0:t}|\tilde{x}_{0:t}^{i,1:N}) = \widehat{p}_{\text{enkf},t}^{(\theta^*)}(y_{0:t}|\tilde{x}_{0:t}^{*,1:N})$ and $x_t^{i,1:N} = x_t^{*,1:N}$.

end if

end for

Output: weighted parameter particles $\{\theta^i, u_t^i\}$, associated ensemble members $x_t^{i,1:N}$ and likelihood evaluations $\widehat{p}_{\text{enkf},t}^{(\theta^i)}(y_{0:t}|\tilde{x}_{0:t}^{i,1:N})$, $i = 1, \ldots, M$.

with θ fixed at an estimate of some central posterior value (e.g. the posterior mean). The value of $\hat{\sigma}_N^2$ can also be used to trigger updating of N, for example, if $\hat{\sigma}_N^2 > 1.5$. We refer the reader to Botha et al. (2023b) for further discussion, noting their critique that, in the SMC^2 setting, this approach can be sensitive to the initial value of N. However, and as discussed at the beginning of this section, $\widehat{p}_{\text{enkf},t}^{(\theta)}(y_{0:t}|\tilde{x}_{0:t}^{1:N})$ is likely to be less sensitive to N than the corresponding particle filter estimator.

4.2 Resample-move: delayed-acceptance kernel

As with SMC^2, the most computationally expensive step of the NEnKF algorithm is the resample-move step; if executed at time t, the cost is $\mathcal{O}(tMN)$. We, therefore, aim to avoid expensive calculation of the likelihood $\widehat{p}_{\text{enkf},t}^{(\theta)}(y_{0:t}|\tilde{x}_{0:t}^{1:N})$ for proposed parameter values that are likely to be rejected. Hence, we propose to replace the standard Metropolis-Hastings move in step 3 of Algorithm 6 with a delayed acceptance (DA) move (*e.g.* Christen and Fox, 2005; Golightly et al., 2015; Banterle et al., 2019).

The DA move requires a surrogate for which we use the (unique) resampled particles and their corresponding log-likelihood evaluations. Given $\{\theta^i, \log \widehat{p}_{\text{enkf}}^{(\theta^i)}(y_{0:t}|\tilde{x}_{0:t}^{i,1:N})\}_{i=1}^{M_r}$, where M_r denotes the number of unique resampled parameter particles, we construct an approximate likelihood for a new parameter value, θ, as follows. We find the k-nearest neighbours of θ, denoted $\theta^{[1]}, \ldots, \theta^{[k]}$, and their associated log-likelihood estimates $\log \widehat{p}_{\text{enkf}}^{(\theta^{[1]})}(y_{0:t}|\tilde{x}_{0:t}^{[1],1:N}), \ldots, \log \widehat{p}_{\text{enkf}}^{(\theta^{[k]})}(y_{0:t}|\tilde{x}_{0:t}^{[k],1:N})$. We then

approximate the log-likelihood via the weighted average

$$\log \widehat{p}^{(\theta)}_{\mathrm{knn},t}(y_{0:t}) = \frac{\sum_{i=1}^{k} d_{[i]}^{-1} \log \widehat{p}^{(\theta^{[i]})}_{\mathrm{enkf},t}(y_{0:t}|\tilde{x}^{[i],1:N}_{0:t})}{\sum_{i=1}^{k} d_{[i]}^{-1}}$$

where $d_{[i]}$ denotes the distance (using some metric) between θ and $\theta^{[i]}$. Note that we suppress explicit dependence of the surrogate on the k-nearest neighbours for notational simplicity.

For a given particle θ^i, Stage One of the DA scheme proposes $\theta^* \sim q(\theta^i, \cdot)$, computes $\widehat{p}^{(\theta^*)}_{\mathrm{knn},t}(y_{0:t})$ and the screening acceptance probability

$$\alpha_1\left(\theta^i, \theta^*\right) = 1 \wedge \frac{\pi(\theta^*)\widehat{p}^{(\theta^*)}_{\mathrm{knn},t}(y_{0:t})}{\pi(\theta^i)\widehat{p}^{(\theta^i)}_{\mathrm{knn},t}(y_{0:t})} \times \frac{q(\theta^*, \theta^i)}{q(\theta^i, \theta^*)}. \tag{19}$$

If this screening step is successful, Stage Two of the DA scheme constructs $\widehat{p}^{(\theta^*)}_{\mathrm{enkf},t}(y_{0:t}|\tilde{x}^{*,1:N}_{0:t})$ and the Stage Two acceptance probability

$$\alpha_{2|1}(\theta^i, \theta^*) = 1 \wedge \frac{\widehat{p}^{(\theta^*)}_{\mathrm{enkf},t}(y_{0:t}|\tilde{x}^{*,1:N}_{0:t})}{\widehat{p}^{(\theta^i)}_{\mathrm{enkf},t}(y_{0:t}|\tilde{x}^{i,1:N}_{0:t})} \times \frac{\widehat{p}^{(\theta^i)}_{\mathrm{knn},t}(y_{0:t})}{\widehat{p}^{(\theta^*)}_{\mathrm{knn},t}(y_{0:t})}. \tag{20}$$

Thus the overall acceptance probability for the scheme is $\alpha_1\alpha_{2|1}$ and standard arguments show that iterating the DA scheme defines a Markov chain that is reversible with respect to the (extended) target $\widehat{\pi}_{\mathrm{enkf},t}(\theta, \tilde{x}^{1:N}_{0:t}, x^{1:N}_{0:t}|y_{0:t})$.

4.3 Nonlinear observation model

It has been assumed that the density, $f_t^{(\theta)}(\cdot|x)$, arising from the observation model is a linear and Gaussian conditional density; see (8). Suppose now that $f_t^{(\theta)}$ can be evaluated point-wise and may be neither linear nor Gaussian. Key to our approach in this scenario is that $f_t^{(\theta)}$ can be approximated by a linear Gaussian conditional density which we denote by $g_t^{(\theta)}(\cdot|x)$ and whose form is given by (8). For example, if $f_t^{(\theta)}(y|x) = \mathcal{N}(y_t; h(x_t), R)$ for some nonlinear function $h(\cdot)$ (which may depend on θ), an approximate density $g_t^{(\theta)}$ can be found be taking the first two terms of a Taylor series expansion of $h(\cdot)$ about the forecast mean $\mu_{t|t}$ (see e.g. Evensen et al., 2022), or by augmenting x_t to include $h(\cdot)$ in the forecast ensemble (see e.g. Anderson, 2001). An example of an appropriate $g_t^{(\theta)}$ in the case of a Gaussian observation model with state-dependent variance can be found in Section 5.2.

We consider first the state estimation problem within the context described above. We denote by $\widetilde{p}^{(\theta)}_{\mathrm{enkf},t}(x_t|y_{0:t}, \tilde{x}^{1:N}_t)$ the filtering density at time t, based on use of the EnKF with a *nonlinear observation model* $f_t^{(\theta)}$. We obtain

$$\widetilde{p}^{(\theta)}_{\mathrm{enkf},t}(x_t|y_{0:t}, \tilde{x}^{1:N}_t) = \frac{\widehat{p}^{(\theta)}_{\mathrm{enkf},t}(x_t|y_{0:t-1}, \tilde{x}^{1:N}_t) f_t^{(\theta)}(y_t|x_t)}{\widetilde{p}^{(\theta)}_{\mathrm{enkf},t}(y_t|y_{0:t-1}, \tilde{x}^{1:N}_t)} \tag{21}$$

which has the same form as (10), but now owing to the nonlinear observation model, the denominator (that is, the observed-data likelihood contribution) $\widetilde{p}^{(\theta)}_{\mathrm{enkf},t}(y_t|y_{0:t-1}, \tilde{x}^{1:N}_t)$ is intractable. The filtering density in (21) can be approximated by replacing $f_t^{(\theta)}$ with the linear and Gaussian approximation $g_t^{(\theta)}$. The resulting approximation is a tractable Gaussian density given by

$$\widehat{g}^{(\theta)}_{\mathrm{enkf},t}(x_t|y_{0:t}, \tilde{x}^{1:N}_t) = \frac{\widehat{p}^{(\theta)}_{\mathrm{enkf},t}(x_t|y_{0:t-1}, \tilde{x}^{1:N}_t) g_t^{(\theta)}(y_t|x_t)}{\widehat{g}^{(\theta)}_{\mathrm{enkf},t}(y_t|y_{0:t-1}, \tilde{x}^{1:N}_t)}. \tag{22}$$

Hence, the denominator $\widehat{g}^{(\theta)}_{\text{enkf},t}(y_t|y_{0:t-1}, \tilde{x}_t^{1:N})$ can be computed analytically using Algorithm 3, for a suitable choice of H and R, deduced from the example specific $g_t^{(\theta)}$. Parameter (and state) filtering may then proceed via the NEnKF (Algorithm 6) at the expense of inferential accuracy, due to the additional error induced by $g_t^{(\theta)}$.

Naturally, inferential accuracy can be maintained at the expense of computational cost, by eschewing the EnKF in favour of the particle filter with target $p_t^{(\theta)}(x_t|y_{0:t})$ given by (3). That is, Algorithm 1 can be run, for example, with a proposal density $q_t^{(\theta)}(x_t|x_{t-1}, y_t) := p_t(x_t|x_{t-1})$. However, particles propagated myopically of the next observation can result in an observed-data likelihood estimator with high variance (Del Moral and Murray, 2015), which can be inefficient when used inside SMC^2 (Golightly and Kypraios, 2018). Methods which use the EnKF as a proposal mechanism inside a particle filter over states have been proposed by Papadakis et al. (2010) (see also Tamboli, 2021; van Leeuwen et al., 2019). In particular, use of $\widehat{g}^{(\theta)}_{\text{enkf},t}(x_t|y_{0:t}, \tilde{x}_t^{1:N})$ in place of $q_t^{(\theta)}(x_t|x_{t-1}^{a_{t-1}^j}, y_t)$ in Algorithm 1 corresponds to the weighted ensemble Kalman filter of Papadakis et al. (2010). One possible implementation of this approach is to take $\widehat{g}^{(\theta)}_{\text{enkf},t}(x_t|y_{0:t}, \tilde{x}_t^{1:N})$ as the density associated with an ensemble member generated by the update step of Algorithm 3, for a suitable choice of H and R, and conditional on the forecast ensemble $\tilde{x}_t^{1:N}$. The weight function then takes the form

$$\tilde{w}_t(\tilde{x}_t^{1:N}, x_{t-1}^{a_{t-1}^j}, x_t^j) = \frac{p_t^{(\theta)}(x_t^j|x_{t-1}^{a_{t-1}^j}) f_t^{(\theta)}(y_t|x_t^j)}{\widehat{g}^{(\theta)}_{\text{enkf},t}(x_t^j|y_{0:t}, \tilde{x}_t^{1:N})}. \tag{23}$$

However, in many scenarios of practical interest, it is beneficial to model states at a finer frequency than at which observations are observed. In this case, the state vector x_t is replaced by the matrix $(x_{t,1}, \ldots, x_{t,m})$, whose elements can be simulated recursively from some kernel $p_{t,i}^{(\theta)}(x_{t,i}|x_{t,i-1})$ such that $p_t^{(\theta)}(x_t|x_{t-1}) = \int \prod_{i=1}^m p_{t,i}^{(\theta)}(x_{t,i}|x_{t,i-1}) dx_{t,1:m-1}$. In this setting, $p_t^{(\theta)}(x_t|x_{t-1})$ can be sampled but not typically evaluated, precluding the use of (23).

We therefore propose a third option, which leverages the inferential accuracy of SMC^2 and the computational efficiency of the EnKF, and can be applied in scenarios where the latent state process is required on a finer time-scale than the observations. Here, the inner loop of SMC^2 operates by using a particle filter over states, with target $\widetilde{p}^{(\theta)}_{\text{enkf},t}(x_t|y_{0:t}, \tilde{x}_t^{1:N})$ given by (21) and a proposal mechanism $\widehat{g}^{(\theta)}_{\text{enkf},t}(x_t|y_{0:t}, \tilde{x}_t^{1:N})$ given by (22). Hence, in Algorithm 1, the propagate step samples $x_t^j \sim \widehat{g}^{(\theta)}_{\text{enkf},t}(x_t|y_{0:t}, \tilde{x}_t^{1:N})$, $j = 1 \ldots, N$, via a single run of Algorithm 3 with inputs θ, resampled particles $x_{t-1}^{a_{t-1}^{1:N}}$ and a suitable choice of H and R. It should be clear that the unnormalised weight of the jth particle x_t^j is given by

$$\begin{aligned}\tilde{w}_t(\tilde{x}_t^{1:N}, x_t^j) &= \frac{\widehat{p}^{(\theta)}_{\text{enkf},t}(x_t^j|y_{0:t-1}, \tilde{x}_t^{1:N}) f_t^{(\theta)}(y_t|x_t^j)}{\widehat{g}^{(\theta)}_{\text{enkf},t}(x_t^j|y_{0:t}, \tilde{x}_t^{1:N})} \\ &= \widehat{g}^{(\theta)}_{\text{enkf},t}(y_t|y_{0:t-1}, \tilde{x}_t^{1:N}) \times \frac{f_t^{(\theta)}(y_t|x_t^j)}{g_t^{(\theta)}(y_t|x_t^j)}\end{aligned} \tag{24}$$

where $\widehat{g}^{(\theta)}_{\text{enkf},t}(y_t|y_{0:t-1}, \tilde{x}_t^{1:N})$ is obtained from the single run of Algorithm 3 in the propagate step. We note that $p_t^{(\theta)}(x_t|x_{t-1})$ is sampled in step 1 of Algorithm 3 when generating the forecast ensemble, but need never be evaluated, since the corresponding forecast density, $\widehat{p}^{(\theta)}_{\text{enkf},t}(x_t|y_{0:t-1}, \tilde{x}_t^{1:N})$, appears in both $\widetilde{p}^{(\theta)}_{\text{enkf},t}(x_t|y_{0:t}, \tilde{x}_t^{1:N})$ and $\widehat{g}^{(\theta)}_{\text{enkf},t}(x_t|y_{0:t}, \tilde{x}_t^{1:N})$, and therefore cancels in the weight

function. This necessarily sacrifices inferential accuracy (compared to targeting $p_t^{(\theta)}(x_t|y_{0:t})$) but allows for integrating x_{t-1} (and $(x_{t,1},\ldots,x_{t,m})$ where relevant) out of the weight function. This procedure is known as Rao-Blackwellisation (RB) and can lead to weights with lower variance (see e.g. Doucet et al., 2000). Finally, taking the average (over state particles $x_t^{1:N}$) of $\tilde{w}_t(\tilde{x}_t^{1:N}, x_t^j)$ in (24) estimates the observed-data likelihood $\widetilde{p}_{\text{enkf},t}^{(\theta)}(y_t|y_{0:t-1}, \tilde{x}_t^{1:N})$, that is, the denominator in (21). Such estimates can be used directly in the SMC^2 scheme (see Algorithm 2) to give recursive exploration of a target which we denote by $\widetilde{\pi}_{\text{enkf},t}(\theta|y_{0:t})$. We refer to the resulting inference scheme for this target as RB-SMC^2.

5 Applications

To illustrate the nested ensemble Kalman filter (NEnKF) and benchmark against existing methods, we consider four applications of increasing complexity. In Section 5.1, we perform inference on an Ornstein-Uhlenbeck model using synthetic data. We compare the performance of NEnKF against the augmented and particle ensemble Kalman filters (AEnKF and PEnKF of Sections 3.3 and 3.4). We additionally benchmark performance and accuracy using the output of an MCMC scheme which directly targets the parameter posterior. In Section 5.2, we apply the NEnKF and two implementations of SMC^2 in the context of a nonlinear observation model, via a stochastic model of predator-prey interaction. Section 5.3 considers a real data example involving the spread of oak processionary moth in south-east England. Finally, in Section 5.4, we consider inference for the parameters governing a 10-dimensional Lorenz-96 model. For the second and final applications, inferential accuracy is benchmarked against the output of a particle MCMC scheme. All algorithms were coded in R and run on a desktop computer with an Intel Core i7-10700 processor and a 2.90GHz clock speed. For the Lorenz 94 application (Section 5.4), the per particle steps corresponding to reweighting, mutation and updating of N were parallelised across 10 cores. The code is available from https://github.com/AndyGolightly/NestedEnKF.

5.1 Ornstein-Uhlenbeck process

Consider a process $\{X_t, t \geq 0\}$ satisfying an Itô stochastic differential equation (SDE) of the form

$$dX_t = \theta_1(\theta_2 - X_t)dt + \theta_3 dW_t$$

where W_t is a standard Brownian motion process. This SDE can be solved analytically to give

$$p(x_{t+\Delta t}|x_t, \theta) = \mathcal{N}\left(x_{t+\Delta t};\, x_t e^{-\theta_1 \Delta t} + \theta_2(1 - e^{-\theta_1 \Delta t}),\, \frac{\theta_3^2}{2\theta_1}(1 - e^{-2\theta_1 \Delta t})\right).$$

Using this solution, we simulated 50 points at integer times from a single realisation of a path using an initial condition of $x_0 = 10$ and $\theta = (1, 2, 1)'$. We then corrupted the resulting skeleton path using the observation model in (8) with $H = 1$ and $R = 0.1$. We adopted an independent prior specification with $\theta_1 \sim \text{Gamma}(2, 2)$, $\theta_2 \sim \text{Gamma}(5, 3)$ and $\theta_3 \sim \text{Gamma}(2, 5)$. In what follows, we assume that the initial condition and observation noise are fixed and known.

We ran NEnKF with $M = 1000$ particles and initial ensemble members $N = 10$. A mutation step was triggered if the effective sample size (6) fell below 400 ($\gamma = 0.4$). Updating of N was triggered following a move step if the estimate $\hat{\sigma}_N^2$ of $\text{Var}[\widehat{p}_{\text{enkf},t}^{(\bar{\theta})}(y_{0:t}|\tilde{x}_{0:t}^{1:N})]$ exceeded 1.5, resulting in the update $\tilde{N} = \hat{\sigma}_N^2 N$. We additionally ran NEnKF with a delayed acceptance kernel in the move step, based on the k-nearest neighbours surrogate of Section 4.2, with $k = 3$. This gave a modest decrease in CPU time of around 10% over NEnKF; therefore all results are based on NEnKF with delayed acceptance.

Scheme	N	M	CPU	Bias (RMSE)					
				$\widehat{\mathrm{E}}(\log\theta_1)$	$\widehat{\mathrm{E}}(\log\theta_2)$	$\widehat{\mathrm{E}}(\log\theta_3)$	$\widehat{\mathrm{SD}}(\log\theta_1)$	$\widehat{\mathrm{SD}}(\log\theta_2)$	$\widehat{\mathrm{SD}}(\log\theta_3)$
NEnKF	100	1000	43	0.0036	-0.0047	0.0003	0.0068	0.0014	0.0003
				(0.031)	(0.010)	(0.021)	(0.019)	(0.005)	(0.010)
PEnKF	100	4000	46	0.0027	-0.0078	0.0037	0.0098	0.0010	-0.0020
				(0.033)	(0.010)	(0.024)	(0.020)	(0.007)	(0.012)
AEnKF	25000	–	50	-0.0861	-0.0396	-0.8898	0.0243	0.0058	0.6795
				(0.020)	(0.006)	(0.068)	(0.004)	(0.004)	(0.005)

Table 1: OU example. Number of ensemble members N (at termination), number of particles M, CPU time (in seconds), bias (and RMSE in parentheses) of estimators of the posterior expectations $\mathrm{E}(\log\theta_i)$ and standard deviations $\mathrm{SD}(\log\theta_i)$, $i = 1, 2, 3$. All results are obtained by averaging over 100 runs of each inference scheme.

We ran PEnKF and AEnKF with respective particle M and ensemble member N values chosen to give a CPU time in approximate agreement with that of NEnKF-DA. For PEnKF, we fixed N at the average value obtained at termination of NEnKF over several replicate runs. Both schemes require choosing the hyper-parameters a and h used in the artificial evolution kernel. We followed Liu and West (2001) by setting $a = \sqrt{1-h^2}$ and $h = 1 - ((3\delta - 1)/2\delta)^2$ with the recommendation that the discount factor δ is around $0.95 - 0.99$. We considered several choices of δ and report results for $\delta = 0.97$, which we found to give best performance.

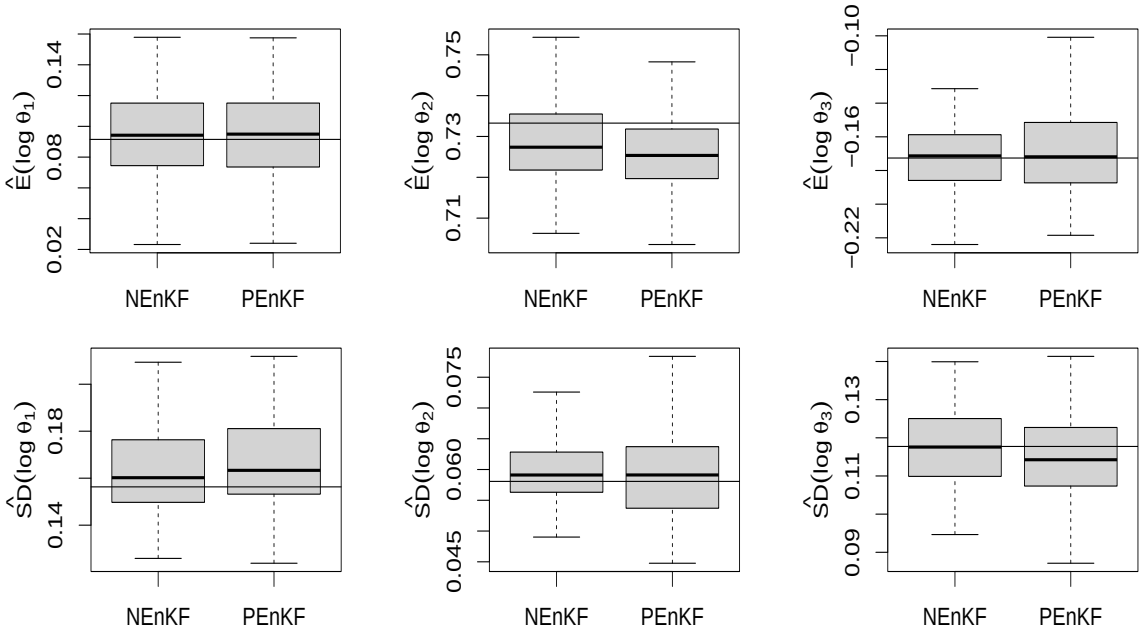

Figure 1: OU example. Distributions of the estimators of posterior expectations $\mathrm{E}(\log\theta_i)$ and standard deviations $\mathrm{SD}(\log\theta_i)$, $i = 1, 2, 3$, under NEnKF with $M = 1000$ and PEnKF with $M = 4000$. The ground truth is indicated by a horizontal line.

Using the settings described above, 100 replicate runs of each scheme were performed, and the results summarised in Table 1 and Figures 1-2. We compare the accuracy of each scheme by reporting bias and root mean square error (RMSE) of the estimators of the marginal posterior means and standard deviations of each $\log\theta_i$. These summaries, denoted $\mathrm{E}(\log\theta_i)$ and $\mathrm{SD}(\log\theta_i)$ respectively, are reported in Table 1 and were obtained by comparing estimates from replicate runs to 'gold standard' reference values, obtained from a long run (10^6 iterations) of an MCMC scheme

targeting the marginal parameter posterior $\pi_T(\theta|y_{0:T})$, as given by (1); for an OU process, the observed-data likelihood $p_T^\theta(y_{0:T})$ is tractable.

There are considerable differences in accuracy of AEnKF compared to NEnKF and PEnKF, with the former consistently over-estimating all posterior quantities of interest. This is particularly noticeable for the marginal posterior mean and standard deviation of $\log \theta_3$, which controls the intrinsic stochasticity of the latent process, and for which an assumed linear Gaussian relationship between this parameter and the observation process is likely to be unsatisfactory. There is comparatively little difference between NEnKF and PEnKF, although Figure 1 suggests that lower bias and RMSE is achieved for NEnKF.

5.2 Lotka-Volterra model

The Lotka-Volterra system admits a bivariate SDE giving a simple description of the time-course behaviour of prey ($X_{1,t}$) and predators ($X_{2,t}$). It has been ubiquitously used to benchmark competing inference algorithms (see e.g. Fuchs, 2013; Ryder et al., 2021; Graham et al., 2022). The SDE takes the form

$$dX_t = a(X_t, \theta)dt + b(X_t, \theta)^{1/2} dW_t \tag{25}$$

where

$$a(X_t, \theta) = \begin{pmatrix} \theta_1 X_{1,t} - \theta_2 X_{1,t} X_{2,t} \\ \theta_2 X_{1,t} X_{2,t} - \theta_3 X_{2,t} \end{pmatrix}, \qquad b(X_t, \theta) = \begin{pmatrix} \theta_1 X_{1,t} + \theta_2 X_{1,t} X_{2,t} & -\theta_2 X_{1,t} X_{2,t} \\ -\theta_2 X_{1,t} X_{2,t} & \theta_2 X_{1,t} X_{2,t} + \theta_3 X_{2,t} \end{pmatrix}.$$

Although this SDE cannot be solved analytically, we adopt a time discretisation approach by partitioning $[t-1, t]$ into $m+1$ equally spaced times $t = t, 0 < t, 1 < \ldots < t, m = t$ with time-step Δt. We then set $p_t^{(\theta)}(x_t|x_{t-1}) = \int \prod_{i=1}^m p_{t,i}^{(\theta)}(x_{t,i}|x_{t,i-1}) dx_{t,1:m-1}$ where $p_{t,i}^{(\theta)}(x_{t,i}|x_{t,i-1})$ is the Euler-Maruyama approximation:

$$p_{t,i}^{(\theta)}(x_{t,i}|x_{t,i-1}) = \mathcal{N}\left(x_{t,i}; x_{t,i-1} + \alpha(x_{t,i-1}, \theta)\Delta t, \beta(x_{t,i-1}, \theta)\Delta t\right). \tag{26}$$

To create a challenging data-poor scenario, we set $X_0 = (50, 50)'$, $\theta = (0.5, 0.0025, 0.3)'$ and recursively sampled (26) over $[0, 40]$ with $\Delta t = 10^{-3}$. The resulting trace was thinned by a factor of 2000, to give 20 observations with equal time spacing of 2 time units. We then discarded predator values and corrupted the remaining prey values according to an observation model of the form

$$f_t^{(\theta)}(y_t|x_t) = \mathcal{N}\left(y_t; Hx_t, Hx_t\right) \tag{27}$$

where $H = (1, 0)$. This (nonlinear) observation model effectively represents a Gaussian approximation to a Poisson model, and has been used in application in population ecology by Lowe and Golightly (2023) among others. Hence, in addition to vanilla SMC^2 (see Section 2.3), we consider use of the EnKF as descsribed in Section 4.3, as appropriate for nonlinear observation models. In more detail, we implemented three schemes as follows:

1. *Nested EnKF* (NEnKF). The target at time t is $\widehat{\pi}_{\text{enkf},t}(\theta|y_{0:t})$. Observed-data likelihood contributions $\widehat{p}_{\text{enkf},t}^{(\theta)}(y_t|y_{0:t-1}, \tilde{x}_t^{1:N})$ are calculated using Algorithm 3 with R replaced by $H\hat{\mu}_{t|t-1}$, permitting a linear Gaussian approximation of (27).

2. *Rao-Blackwellised SMC*^{2} (RB-SMC^2). The target at time t is $\widetilde{\pi}_{\text{enkf},t}(\theta|y_{0:t})$. Estimates of observed-data likelihood contributions $\widetilde{p}_{\text{enkf},t}^{(\theta)}(y_t|y_{0:t-1}, \tilde{x}_t^{1:N})$ are calculated using Algorithm 1, with weight function (24) where $f_t^{(\theta)}(y_t|x_t)$ is given by (27), $g_t^{(\theta)}(y_t|x_t) = \mathcal{N}(y_t, Hx_t, R)$ and $\widehat{g}_{\text{enkf},t}^{(\theta)}(y_t|y_{0:t-1}, \tilde{x}_t^{1:N})$ is obtained by running Algorithm 3, with $R = H\hat{\mu}_{t|t-1}$. To mitigate against a proposal distribution (for generating x_t^j in Algorithm 1) that is potentially light-tailed compared to the target (21), we scaled $R = H\hat{\mu}_{t|t-1}$ by a factor of 2.

Scheme	N	CPU	Bias (RMSE)					
			$\widehat{\mathrm{E}}(\log\theta_1)$	$\widehat{\mathrm{E}}(\log\theta_2)$	$\widehat{\mathrm{E}}(\log\theta_3)$	$\widehat{\mathrm{SD}}(\log\theta_1)$	$\widehat{\mathrm{SD}}(\log\theta_2)$	$\widehat{\mathrm{SD}}(\log\theta_3)$
NEnKF	20	129	0.0033	-0.0128	-0.0201	-0.0021	-0.0020	-0.0009
			(0.019)	(0.024)	(0.029)	(0.009)	(0.011)	(0.011)
RB-SMC^2	40	287	0.0040	-0.0089	-0.0097	-0.0054	-0.0058	-0.0042
			(0.021)	(0.020)	(0.021)	(0.012)	(0.013)	(0.014)
SMC^2	88	561	0.0047	-0.0015	0.0024	-0.0073	-0.0066	-0.0033
			(0.016)	(0.020)	(0.024)	(0.009)	(0.011)	(0.012)

Table 2: LV example. Number of ensemble members N (at termination), CPU time (in seconds), bias (and RMSE in parentheses) of estimators of the posterior expectations $\mathrm{E}(\log\theta_i)$ and standard deviations $\mathrm{SD}(\log\theta_i)$, $i = 1, 2, 3$. All results are obtained by averaging over 50 runs of each inference scheme with $M = 1000$ parameter particles.

3. *Vanilla SMC*^{2} (SMC^2). The target at time t is $\pi_t(\theta|y_{0:t})$. Estimates of observed-data likelihood contributions $p_t^{(\theta)}(y_t|y_{0:t-1})$ are calculated using Algorithm 1, with step 1. replaced by sampling $x_t^j \sim p_t^{(\theta)}(\cdot|x_{t-1}^{a_{t-1}^j})$ via recursive application of the Euler-Maruyama discretisation. The weight function then becomes $\tilde{w}_t(x_{t-1}^{a_{t-1}^j}, x_t^j) = f_t^{(\theta)}(y_t|x_t^j)$.

An independent prior specification with $\theta_1 \sim \mathrm{Gamma}(2, 4)$, $\theta_2 \sim \mathrm{Gamma}(20, 10^4)$ and $\theta_3 \sim \mathrm{Gamma}(2, 4)$ was adopted. We then ran the above schemes with $M = 1000$ particles and initial ensemble members $N = 20$. Sampling from $p_t^{(\theta)}(x_t|x_{t-1})$ used (26) with $\Delta t = 0.2$. The conditions for triggering a resample-move step and increasing N were as outlined in Section 5.1. All schemes used a delayed acceptance kernel in the move step, based on the k-nearest neighbours surrogate of Section 4.2, with $k = 3$. This gave a decrease in CPU time of around 30% over the corresponding schemes which used a standard (pseudo-marginal) MH kernel.

Using the settings described above, 50 replicate runs of each scheme were performed, and the results summarised in Table 2 and Figure 3. We again compare the accuracy of each scheme by reporting bias and root mean square error (RMSE) of the estimators of the marginal posterior means and standard deviations of each $\log\theta_i$. For this application, we computed reference values of these quantities from a long run (10^6 iterations with 100 state particles) of particle MCMC (see *e.g.* Golightly and Wilkinson, 2011, for an application of this scheme to the Lotka-Volterra SDE). Hence, for this application, we report accuracy with reference to the 'ground truth' marginal parameter posterior $\pi_T(\theta|y_{0:T})$, which is also the target of vanilla SMC^2, albeit using a particle filter.

Table 2 reports, *inter alia*, average run times and the average number of ensemble members at termination of each scheme. NEnKF is around a factor of 4 quicker than vanilla SMC^2 and around a factor of 2 quicker than RB-SMC^2, with the latter twice as fast as vanilla SMC^2. However, NEnKF uses a misspecified variance: recall that NEnKF uses the forecast mean to approximate the observation variance Hx_t at time t. Consequently, there are some substantive differences in accuracy between the NEnKF output and gold standard posterior reference values. From Figures 3, it is clear that for NEnKF, estimates of the parameter posterior means are shifted downward for θ_2 and θ_3; there is relatively little difference in estimated posterior standard deviations for each scheme. RB-SMC^2 is able to alleviate these differences in estimated posterior means, giving estimated posterior quantities that are broadly consistent with reference values, albeit with greater computational effort than NEnKF.

5.3 Two-node epidemic model

We consider here a two-node compartmental epidemic model to characterise the spread of oak processionary moth (OPM) in two London parks (Bushy Park and Richmond Park). Similar to Wadkin et al. (2023), we specify a stochastic susceptible-infected-removed (SIR) model (*e.g.* Andersson and Britton, 2000) for each node (park), with common removal rate γ and infestation 'pressure' from the neighbouring node, described by the parameters α_{ij}, where α_{12} is the pressure applied by node 1 (Bushy) on node 2 (Richmond), and α_{21} is the pressure from node 2 on node 1. Unlike Wadkin et al. (2023), we allow time-varying infestation rates $\beta_{1,t}$ and $\beta_{2,t}$ at each node, described by two independent Brownian motion processes, scaled by a common parameter σ_β. The model takes the form of (25), with $X_t = (S_{1,t}, I_{1,t}, S_{2,t}, I_{2,t}, \log\beta_{1,t}, \log\beta_{2,t})'$ and $\theta = (\gamma, \alpha_{1,2}, \alpha_{2,1}, \sigma_\beta)'$. The drift and diffusion functions are given by

$$a(X_t,\theta) = \begin{pmatrix} -\beta_{1,t}(I_{1,t}+\alpha_{21}I_{2,t})S_{1,t} \\ \beta_{1,t}(I_{1,t}+\alpha_{21}I_{2,t})S_{1,t} - \gamma I_{1,t} \\ -\beta_{2,t}(I_{2,t}+\alpha_{12}I_{1,t})S_{2,t} \\ \beta_{2,t}(I_{2,t}+\alpha_{12}I_{1,t})S_{2,t} - \gamma I_{2,t} \\ 0 \\ 0 \end{pmatrix}, \qquad b(X_t,\theta) = \mathrm{diag}\{b_{11}, b_{22}, b_{33}\}$$

where

$$b_{11} = \begin{pmatrix} \beta_{1,t}(I_{1,t}+\alpha_{21}I_{2,t})S_{1,t} & -\beta_{1,t}(I_{1,t}+\alpha_{21}I_{2,t})S_{1,t} \\ -\beta_{1,t}(I_{1,t}+\alpha_{21}I_{2,t})S_{1,t} & \beta_{1,t}(I_{1,t}+\alpha_{21}I_{2,t})S_{1,t} + \gamma I_{1,t} \end{pmatrix},$$

$$b_{22} = \begin{pmatrix} \beta_{2,t}(I_{2,t}+\alpha_{12}I_{1,t})S_{2,t} & -\beta_{2,t}(I_{2,t}+\alpha_{12}I_{1,t})S_{2,t} \\ -\beta_{2,t}(I_{2,t}+\alpha_{12}I_{1,t})S_{2,t} & \beta_{2,t}(I_{2,t}+\alpha_{12}I_{1,t})S_{2,t} + \gamma I_{2,t} \end{pmatrix}$$

and $b_{33} = \sigma_\beta^2$.

The data (see Figure 5) consist of (noisy) observations of removal prevalence $(R_{1,t}, R_{2,t})'$, that is, the cumulative numbers of tree locations where nest removal has taken place, observed each year over the period 2013-2024. We assume a fixed number of tree locations (N_j) at each node j so that $S_{j,t} + I_{j,t} + R_{j,t} = \mathrm{N}_j$, $j = 1, 2$, and observation of removals is equivalent to observation of the sums $S_{1,t} + I_{1,t}$ and $S_{2,t} + I_{2,t}$. Following Wadkin et al. (2023), we specify an observation model with density

$$f_t^{(\theta)}(y_t|x_t) = \mathcal{N}\left(y_t; Hx_t, \sigma^2\mathrm{diag}\{Hx_t\}\right) \tag{28}$$

where

$$H = \begin{pmatrix} 1 & 1 & 0 & 0 & 0 & 0 \\ 0 & 0 & 1 & 1 & 0 & 0 \end{pmatrix}.$$

We assume that σ is unknown and append it to the parameter vector θ.

We adopted an independent prior specification with Gamma$(2, 2)$, for all parameter components except σ_β, for which we ascribed a Gamma$(2, 10)$ distribution, reflecting our prior belief that the intrinsic stochasticity in the infestation process is small, relative to the observation noise. We ran NEnKF and RB-SMC^2, both of which use Algorithm 3, which requires a linear Gaussian approximation of (28). For NEnF, we used $R = \sigma^2\mathrm{diag}\{H\hat{\mu}_{t|t-1}\}$; for RB-SMC^2, this quantity was further scaled by a factor of 2. We performed a single run of these schemes with $M = 20,000$ particles and $N = 20$ initial ensemble members. An initial condition of $x_0 = (4631, 240, 37413, 1400, -10, -10.5)'$ was assumed to be fixed and known for each run. We followed Section 5.2 by sampling $p_t^{(\theta)}(x_t|x_{t-1})$ through recursive draws of the Euler-Maruyama approximation (26) with $\Delta t = 0.1$. The conditions for triggering a resample-move step and increasing N were as Section 5.1. Both schemes used a delayed acceptance kernel in the move step (with $k = 3$), which gave a decrease in CPU time of

approximately 15% for NEnKF and 25% for RB-SMC^2, over use of a standard (pseudo-marginal) MH kernel.

The output of NEnKF and RB-SMC^2 is summarised in Figures 4 and 5. The former shows good agreement in posterior output from both schemes while the latter shows that the model can generate predicted removal prevalences that are consistent with the data, and that the infestation rates are plausibly constant. NEnKF terminated with $N = 85$ ensemble members, whereas RB-SMC^2 terminated with $N = 300$, giving a relative CPU cost of roughly 1:2.7. It is worth noting here that computational resources precluded running vanilla SMC^2. A typical termination value of N for SMC^2 can be determined by requiring $\mathrm{Var}[\widehat{p}_T^{(\bar{\theta})}(y_{0:T}|x_{0:T}^{1:N}, a_{0:T-1}^{1:N})] \approx 1.5$, where $\bar{\theta}$ is the parameter posterior mean estimated from RB-SMC^2. This gave $N \approx 5,000$, underlining the benefit of propagating the latent state process conditional on the next observation (as in NEnKF and RB-SMC^2) as opposed to myopically (as in vanilla SMC^2).

5.4 Lorenz 96

Consider a process $\{X_t, t \geq 0\}$ satisfying the Itô SDE

$$dX_t = a(X_t, \theta)dt + \Sigma^{1/2}dW_t. \tag{29}$$

Here, the drift $a(X_t, \theta)$ is a length-d vector with ith component

$$a_i(X_t, \theta) = \theta_1(X_{i+1,t} - X_{i-2,t})X_{i-1,t} - \theta_2 X_{i,t} + \theta_3$$

with addition and subtraction of component indices interpreted modulo d. The diffusion matrix is a diagonal matrix such that $\Sigma = \theta_4^2 I_{d\times d}$. This SDE can be seen as a stochastic representation of the Lorenz 96 dynamical system (Lorenz, 1996), and is often used for benchmarking inference schemes in high-dimensional settings. Following Drovandi et al. (2022), we set $x_0 = (0, \ldots, 0)'$ and $\theta = (1, 1, 8, \sqrt{10})'$. Two synthetic data sets, $\mathcal{D}_1$ (with $d = 5$) and $\mathcal{D}_2$ (with $d = 10$), were generated via recursive sampling of the Euler-Maruyama approximation of (29) over $[0, 30]$ with $\Delta t = 5\times 10^{-3}$. The resulting paths were thinned by a factor of 40 and corrupted with additive Gaussian noise, with zero mean and variance $R = 5^2 I_{d\times d}$, giving, for each of $\mathcal{D}_1$ and $\mathcal{D}_2$, 30 observations with an inter-observation time of 0.2 time units.

We adopted an independent prior specification with $\theta_1 \sim \mathrm{Gamma}(4, 4)$, $\theta_2 \sim \mathrm{Gamma}(4, 4)$, $\theta_3 \sim \mathrm{Gamma}(6, 2)$ and $\theta_4 \sim \mathrm{Gamma}(16, 2)$. We implemented NEnKF and SMC^2 with $M = 1000$ particles and initial ensemble members $N = 20$ for data set $\mathcal{D}_1$ and $N = 50$ for data set $\mathcal{D}_2$. Sampling from $p_t^{(\theta)}(x_t|x_{t-1})$ used the Euler-Maruyama approximation of (29) with $\Delta t = 5 \times 10^{-3}$. The conditions for triggering a resample-move step and increasing N were as outlined in Section 5.1. Both schemes used a delayed acceptance kernel in the move step, based on the k-nearest neighbours surrogate of Section 4.2, with $k = 3$. We found that performing 5 iterations of the move step (per parameter particle) was necessary to give adequate parameter rejuvenation for this particular application, likely due to the calculation of particularly small ESS values at some time points, in turn resulting in a surrogate with relatively poor accuracy for some proposed parameter values.

Using the settings described above, 50 replicate runs of both schemes were performed for data set $\mathcal{D}_1$, and the results summarised in Table 3, with accuracy of various posterior estimators compared to reference values computed from particle MCMC (10^6 iterations with 300 state particles). We were unable to repeat this process for data set $\mathcal{D}_2$; in particular running SMC^2 and particle MCMC require around $4,000-5,000$ state particles, precluding replicate runs of SMC^2 and particle MCMC. For this data set, we compare efficiency of SMC^2 and NEnKF via a single run with $M = 5,000$ parameter particles; see Figures 6–7.

Scheme	N	CPU	Bias (RMSE)					
			$\widehat{\mathrm{E}}(\log\theta_1)$	$\widehat{\mathrm{E}}(\log\theta_2)$	$\widehat{\mathrm{E}}(\log\theta_3)$	$\widehat{\mathrm{SD}}(\log\theta_1)$	$\widehat{\mathrm{SD}}(\log\theta_2)$	$\widehat{\mathrm{SD}}(\log\theta_3)$
NEnKF	128	14	0.2082	-0.1804	0.1494	0.0759	0.1465	-0.0064
			(0.263)	(0.277)	(0.120)	(0.105)	(0.149)	(0.043)
SMC^2	450	56	0.2109	-0.1709	0.1158	0.0500	0.0816	0.0084
			(0.170)	(0.205)	(0.098)	(0.044)	(0.109)	(0.043)

Table 3: Lorenz 96 example. Number of ensemble members N (at termination), CPU time (in minutes), bias (and RMSE in parentheses) of estimators of the posterior expectations $\mathrm{E}(\log\theta_i)$ and standard deviations $\mathrm{SD}(\log\theta_i)$, $i = 1, 2, 3$. All results are obtained by averaging over 50 runs of each inference scheme with $M = 1000$ parameter particles using data set $\mathcal{D}_1$ ($d = 5$).

Inspection of Table 3 and Figure 7 suggests that the NEnKF is able to give inferences consistent with SMC^2 and the ground truth parameter values that generated the data. For data set $\mathcal{D}_1$ ($d = 5$), fewer ensemble members are required for NEnKF compared to state particles for SMC^2, leading to an increase in computational efficiency of around a factor of 3.5. For data set $\mathcal{D}_2$ ($d = 10$) and a single run of each scheme, SMC^2 required 4762 state particles whereas NEnKF required just 249 ensemble members, leading to a difference in computational efficiency of approximately a factor of 19 (2737 minutes versus 147 minutes, for SMC^2 versus NEnKF). Not surprisingly, as the observation dimension increases, both schemes require increased numbers of state particles / ensemble members, N, although the relative increase is much smaller when using NEnKF. It is evident from Figure 7, that NEnKF triggers the resample-move and dynamic increasing of N steps less often than SMC^2. When the latter is triggered, realisations of $\hat{\sigma}_N^2$ are typically smaller for NEnKF than SMC^2.

6 Discussion

Bayesian filtering for state-space models in the presence of unknown static parameters is a challenging problem. Sequential Monte Carlo algorithms must overcome particle degeneracy; one such scheme that deals with static parameters in a principled way is the SMC^2 scheme of Chopin et al. (2013). Here, parameter particles are weighted by an estimate of the current observed-data likelihood and, subject to some degeneracy criterion, mutated via a (pseudo-marginal) Metropolis-Hastings kernel which has the marginal parameter posterior as its invariant distrubution. A particle filter over the latent state process is used to estimate the required observed-data likelihood contributions. However, use of the particle filter in this way is likely computationally prohibitive in high-dimensional observation settings, due to requiring that the number of state particles be scaled exponentially with dimension. On the other hand, the ensemble Kalman filter (EnKF, Evensen, 1994) shifts particles (known as ensemble members in the EnKF context) via suitable Gaussian approximations, thus avoiding resampling altogether. Consequently, there is now a vast literature demonstrating the empirical performance of the EnKF for high-dimensional state-space models (see *e.g.* Katzfuss et al., 2019, and the references therein).

We have proposed to use the EnKF within the principled framework of SMC^2 by weighting parameter particles by the EnKF likelihood and, when necessary, mutating these particles by using a Metropolis-Hastings step that again uses the EnKF likelihood. Extensions to the resulting *nested EnKF (NEnKF)* algorithm were considered. In particular, the computational cost of the mutation step can be lessened by screening proposed moves using a surrogate, computed locally using the most recent parameter samples and their likelihood evaluations. As with the simplest implementation of SMC^2, NEnKF is plug-and-play, since only forward simulation of the latent state process and evaluation of the observation density are required. We found, across four applications of increasing

observation dimension, that the NEnKF is able to provide accurate and computationally efficient inferences regarding the static parameters. Since the NEnKF combines a particle filter over parameters with an ensemble Kalman filter over states, we anticipate (and as evidenced by our numerical experiments) greatest utility of the proposed algorithm in settings where the number of observed dynamic components is large compared to the number of parameters to be estimated (*e.g.* $d_\theta < 10$ and $d_y > 10$). The simplest implementation of the NEnKF assumes a linear Gaussian observation model. In scenarios where this assumption is unreasonable, we have proposed to replace the EnKF with a particle filter that uses the EnKF to propagate state particles. Unlike related approaches (*e.g.* Papadakis et al., 2010), we also use the EnKF to give a linear Gaussian approximation of the transition density $p_t^{(\theta)}(x_t|x_{t-1})$, leading to a simple form of weight function that can be readily applied in settings where states are modelled at a finer frequency than observations (as is the case, for example, when working with discretised SDEs).

This work can be extended in a number of ways. For example, in our applications of the delayed acceptance kernel, the number of distinct parameter particles M_r used to construct the k-nn surrogate was typically small (no more than a few thousand particles), justifying an $\mathcal{O}(M_r)$ list look-up method for finding the k-nearest neighbours of each θ^*. Using a variation of the KD-tree (*e.g.* Sherlock et al., 2017) requires $\mathcal{O}(d_\theta \log M_r)$ operations and provides a cheaper alternative to the list look-up method, provided d_θ is moderate. It may also be possible to improve computational efficiency of the NEnKF by adaptively choosing between a delayed-acceptance kernel and standard M-H kernel, when the resample-move step is triggered. For example, in the early phase of the NEnKF scheme, calculating an observed-data likelihood estimator is likely to be relatively cheap. Similar approaches have been considered in the context of IBIS (Fearnhead and Taylor, 2013) and SMC^2 (Botha et al., 2023a). Finally, using the surrogate in both the weighting and resample-move steps (for a fixed value of N) could provide a fixed cost alternative to the NEnKF, to the detriment of inferential accuracy.

References

Agapiou, S., Papaspiliopoulos, O., Sanz-Alonso, D., and Stuart, A. M. (2017). Importance sampling: computational complexity and intrinsic dimension. *Statistical Science*, 32(3):405–431.

Anderson, J. L. (2001). An ensemble adjustment Kalman filter for data assimilation. *Monthly Weather Review*, 129:2884–2903.

Andersson, H. k. and Britton, T. (2000). *Stochastic epidemic models and their statistical analysis*, volume 151 of *Lecture Notes in Statistics*. Springer-Verlag, New York.

Andrieu, C., Doucet, A., and Holenstein, R. (2010). Particle Markov chain Monte Carlo methods. *Journal of the Royal Statistical Society: Series B (Statistical Methodology)*, 72(3):269–342.

Andrieu, C. and Roberts, G. O. (2009). The pseudo-marginal approach for efficient Monte Carlo computations. *The Annals of Statistics*, 37(2):697–725.

Banterle, M., Grazian, C., Lee, A., and Robert, C. P. (2019). Accelerating Metropolis-Hastings algorithms by delayed acceptance. *Foundations of Data Science*, 1:103–128.

Bi, H., Ma, J., and Wang, F. (2015). An improved particle filter algorithm based on ensemble Kalman filter and Markov chain Monte Carlo method. *IEEE Journal of selected topics in earth observations and remote sensing*, 8(2).

Botha, I., Kohn, R., South, L., and Drovandi, C. (2023a). Adaptively switching between a particle marginal metropolis-hastings and a particle Gibbs kernel in SMC^2. *arXiv preprint arXiv:2307.11553*.

Botha, I., Kohn, R., South, L., and Drovandi, C. (2023b). Automatically adapting the number of state particles in SMC^2. *Statistics and Computing*, 33(82).

Carter, C. K. and Kohn, R. (1994). On Gibbs sampling for state space models. *Biometrika*, 81(3):541–553.

Chopin, N. (2002). A sequential particle filter method for static models. *Biometrika*, 89(3):539–552.

Chopin, N., Jacob, P. E., and Papaspiliopoulos, O. (2013). SMC^2: an efficient algorithm for sequential analysis of state space models. *Journal of the Royal Statistical Society: Series B (Statistical Methodology)*, 75(3):397–426.

Christen, J. A. and Fox, C. (2005). Markov Chain Monte Carlo using an approximation. *Journal of Computational and Graphical Statistics*, 14:795–810.

Del Moral, P. (2004). *Feynman-Kac formulae*. Springer.

Del Moral, P., Doucet, A., and Jasra, A. (2006). Sequential Monte Carlo samplers. *Journal of the Royal Statistical Society Series B: Statistical Methodology*, 68(3):411–436.

Del Moral, P. and Murray, L. M. (2015). Sequential Monte Carlo with highly informative observations. *SIAM/ASA Journal on Uncertainty Quantification*, 3(1):969–997.

Doucet, A., de Freitas, N., Murphy, K. P., and Russell, S. J. (2000). Rao-Blackwellised particle filtering for dynamic Bayesian networks. In *Proceedings of the 16th Conference on Uncertainty in Artificial Intelligence*, pages 176–183.

Doucet, A. and Johansen, A. M. (2011). A tutorial on particle filtering and smoothing: Fifteen years later. In Crisan, D. and Rozovskii, B., editors, *Handbook of nonlinear filtering*, pages 656–704. Oxford University Press.

Drovandi, C., Everitt, R. G., Golightly, A., and Prangle, D. (2022). Ensemble MCMC: Accelerating pseudo-marginal MCMC for state space models using the ensemble Kalman filter. *Bayesian Analysis*, 17(1):223–260.

Duan, J.-C. and Fulop, A. (2015). Density-tempered marginalized sequential Monte Carlo samplers. *Journal of Business & Economic Statistics*, 33(2):192–202.

Evensen, G. (1994). Sequential data assimilation with a nonlinear quasi-geostrophic model using Monte Carlo methods to forecast error statistics. *Journal of Geophysical Research*, 99:10143–10162.

Evensen, G. (2009). *Data Assimilation: The Ensemble Kalman Filter*. Springer.

Evensen, G., Vossepoel, F. C., and van Leeuwen, P. J. (2022). *Data Assimilation Fundamentals: A Unified Formulation of the State and Parameter Estimation Problem*. Springer.

Fearnhead, P. and Taylor, B. M. (2013). An Adaptive Sequential Monte Carlo Sampler. *Bayesian Analysis*, 8(2):411 – 438.

Frei, M. and Künsch, H. R. (2011). Sequential state and observation noise covariance estimation using combined ensemble Kalman and particle filters. *Monthly Weather Review*, 140:1476–1495.

Frühwirth-Schnatter, S. (1994). Data augmentation and dynamic linear models. *Journal of time series analysis*, 15(2):183–202.

Fuchs, C. (2013). *Inference for diffusion processes with applications in Life Sciences*. Springer, Heidelberg.

Gamerman, D. and Lopes, H. (2006). *Markov chain Monte Carlo: Stochastic Simulation for Bayesian Inference, Second Edition (2nd ed.)*. Chapman and Hall/CRC.

Gilks, W. R. and Berzuini, C. (2001). Following a moving target – Monte Carlo inference for dynamic Bayesian models. *J. R. Statist. Soc. A.*, 63:127–146.

Golightly, A., Henderson, D. A., and Sherlock, C. (2015). Delayed acceptance particle MCMC for exact inference in stochastic kinetic models. *Statistics and Computing*, 25:1039–1055.

Golightly, A. and Kypraios, T. (2018). Efficient SMC^2 schemes for stochastic kinetic models. *Statistics and Computing*, 28:1215–1230.

Golightly, A. and Wilkinson, D. J. (2011). Bayesian parameter inference for stochastic biochemical network models using particle Markov chain Monte Carlo. *Interface Focus*, 1(6):807–820.

Gordon, N. J., Salmond, D. J., and Smith, A. F. M. (1993). Novel approach to nonlinear/non-Gaussian Bayesian state estimation. *IEE Proceedings F (Radar and Signal Processing)*, 140(2):107–113.

Graham, M. M., Thiery, A. H., and Beskos, A. (2022). Manifold Markov chain Monte Carlo methods for Bayesian inference in diffusion models. Available from `http://arxiv.org/abs/1912.02982`.

Harvey, A. (1990). *Forecasting, Structural Time Series Models and the Kalman Filter*. Cambridge University Press.

Jacob, P. (2015). Sequential Bayesian inference for implicit hidden Markov models and current limitations. *ESAIM: Proceedings and Surveys*, 51:24–48.

Kalman, R. (1960). A new approach to linear filtering and prediction problems. *Journal of Basic Engineering*, 82:35–45.

Katzfuss, M., Stroud, J. R., and Wikle, C. K. (2016). Understanding the ensemble Kalman filter. *The American Statistician*, 70(4):350–357.

Katzfuss, M., Stroud, J. R., and Wikle, C. K. (2019). Ensemble Kalman methods for high-dimensional hierarchical dynamic space-time models. *Journal of the American Statistical Association*, 115:866–885.

Liu, J. and West, M. (2001). Combined parameter and state estimation in simulation-based filtering. In Doucet, A., de Freitas, N., and Gordon, N., editors, *Sequential Monte Carlo Methods in Practice*. New York: Springer.

Lorenz, E. N. (1996). Predictability: A problem partly solved. In *Proc. Seminar on Predictability*.

Lowe, T. E. and Golightly, A. (2023). Accelerating inference for stochastic kinetic models. *Computational Statistics and Data Analysis*, 185:107760.

Mitchell, L. and Arnold, A. (2021). Analyzing the effects of observation function selection in ensemble Kalman filtering for epidemic models. *Mathematical Biosciences*, 339:108655.

Papadakis, N., Mémin, E., Cuzol, A., and Gengembre, N. (2010). Data assimilation with the weighted ensemble Kalman filter. *Tellus A: Dynamic Meteorology and Oceanography*, 62(5):673–697.

Petris, G., Petrone, S., and Campagnoli, P. (2009). Dynamic linear models. In *Dynamic Linear Models with R*, pages 31–84. Springer.

Pitt, M. K., dos Santos Silva, R., Giordani, P., and Kohn, R. (2012). On some properties of Markov chain Monte Carlo simulation methods based on the particle filter. *Journal of Econometrics*, 171(2):134–151.

Ruckstuhl, Y. M. and Janjić, T. (2018). Parameter and state estimation with ensemble Kalman filter based algorithms for convective-scale applications. *Quarterly Journal of the Royal Meteorological Society*, 144(712):826–841.

Ryder, T., Prangle, D., Golightly, A., and Matthews, I. (2021). The neural moving average model for scalable variational inference of state space models. In *Proceedings of the Thirty-Seventh Conference on Uncertainty in Artificial Intelligence*, volume 161 of *Proceedings of Machine Learning Research*, pages 12–22. PMLR.

Särkkä, S. (2013). *Bayesian filtering and smoothing*. Cambridge University Press.

Sherlock, C., Golightly, A., and Henderson, D. A. (2017). Adaptive, delayed-acceptance MCMC for targets with expensive likelihoods. *Journal of Computational and Graphical Statistics*, 26(2):434–444.

Sherlock, C., Thiery, A. H., Roberts, G. O., and Rosenthal, J. S. (2015). On the efficiency of pseudo-marginal random walk Metropolis algorithms. *The Annals of Statistics*, 43(1):238–275.

Shumway, R. H. and Stoffer, D. S. (2006). *Time Series Analysis and its Applications With R Examples*. Springer, 2nd edition.

Stroud, J. R., Katzfuss, M., and Wikle, C. K. (2018). A Bayesian adaptive ensemble Kalman filter for sequential state and parameter estimation. *Monthly Weather Review*, 146:373–386.

Tamboli, P. (2021). An efficient particle filtering algorithm based on ensemble Kalman filter proposal density. Available from `http://10.36227/techrxiv.14813586.v1`.

van Leeuwen, P. J., Künsch, H. R., Nerger, L., Potthast, R., and Reich, S. (2019). Particle filters for high-dimensional geoscience applications: A review. *Quarterly Journal of the Royal Meteorological Society*, 145(723):2335–2365.

Vieira, R. and Wilkinson, D. J. (2016). Online state and parameter estimation in dynamic generalised linear models. Available from `http://arxiv.org/pdf/1608.08666.pdf`.

Wadkin, L. E., Golightly, A., Branson, J., Hoppit, A., Parker, N. G., and Baggaley, A. W. (2023). Quantifying invasive pest dynamics through inference of a two-node epidemic network model. *Diversity*, 15(4).

West, M. and Harrison, J. (2006). *Bayesian forecasting and dynamic models*. Springer Science & Business Media.

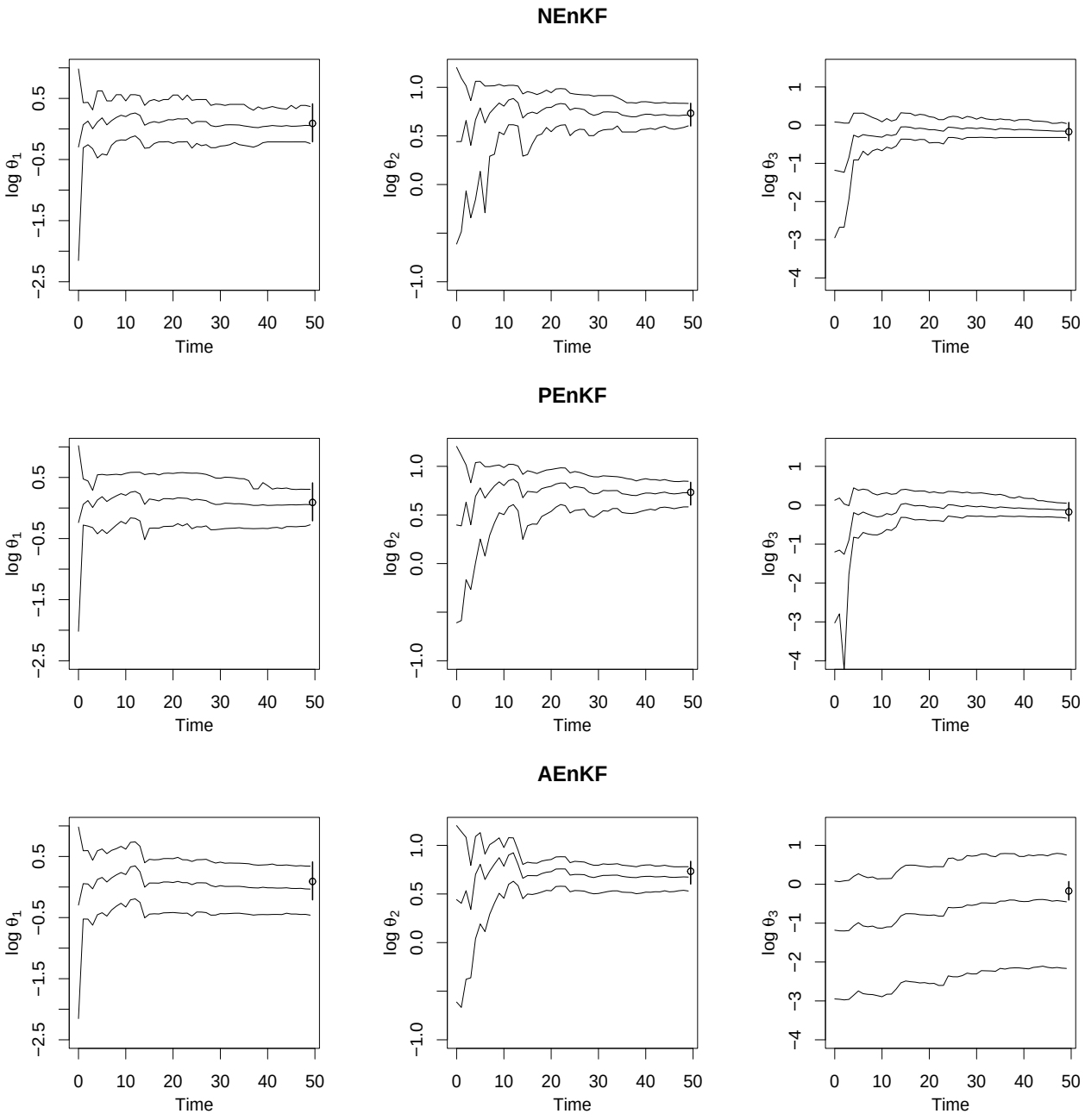

Figure 2: OU example. Marginal parameter filtering means and 95% credible intervals under the NEnKF, PEnKF and AEnKF schemes. For reference, ground truth summaries obtained from the output of eMCMC are displayed at time 49.

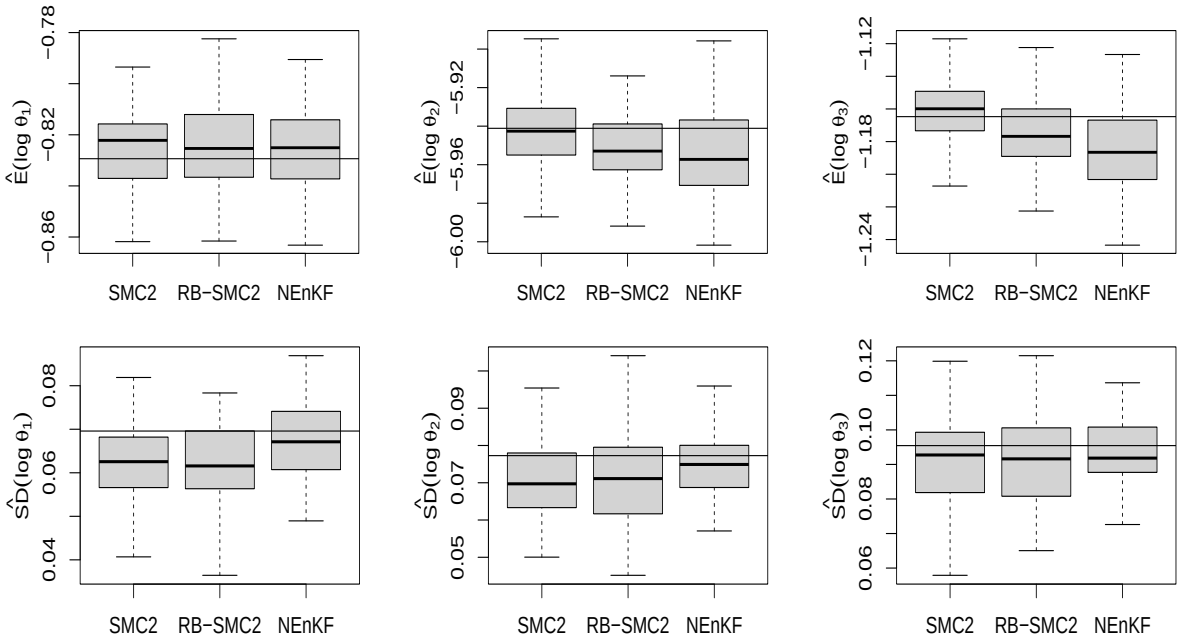

Figure 3: LV example. Distributions of the estimators of posterior expectations $\mathrm{E}(\log \theta_i)$ and standard deviations $\mathrm{SD}(\log \theta_i)$, $i = 1, 2, 3$, SMC^2, RB-SMC^2 and NEnKF, each with $M = 1000$. The ground truth is indicated by a horizontal line.

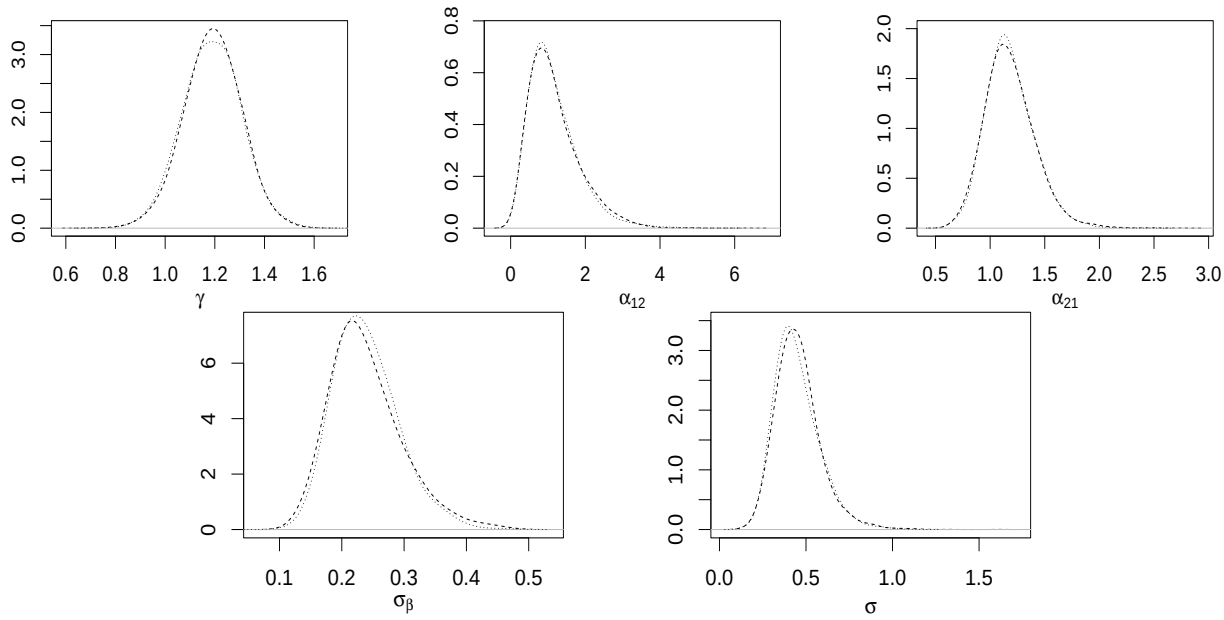

Figure 4: Two-node epidemic example. Marginal parameter posterior distributions at time T from the output of RB-SMC^2 (dotted line) and NEnKF (dashed line) using $M = 5 \times 10^4$.

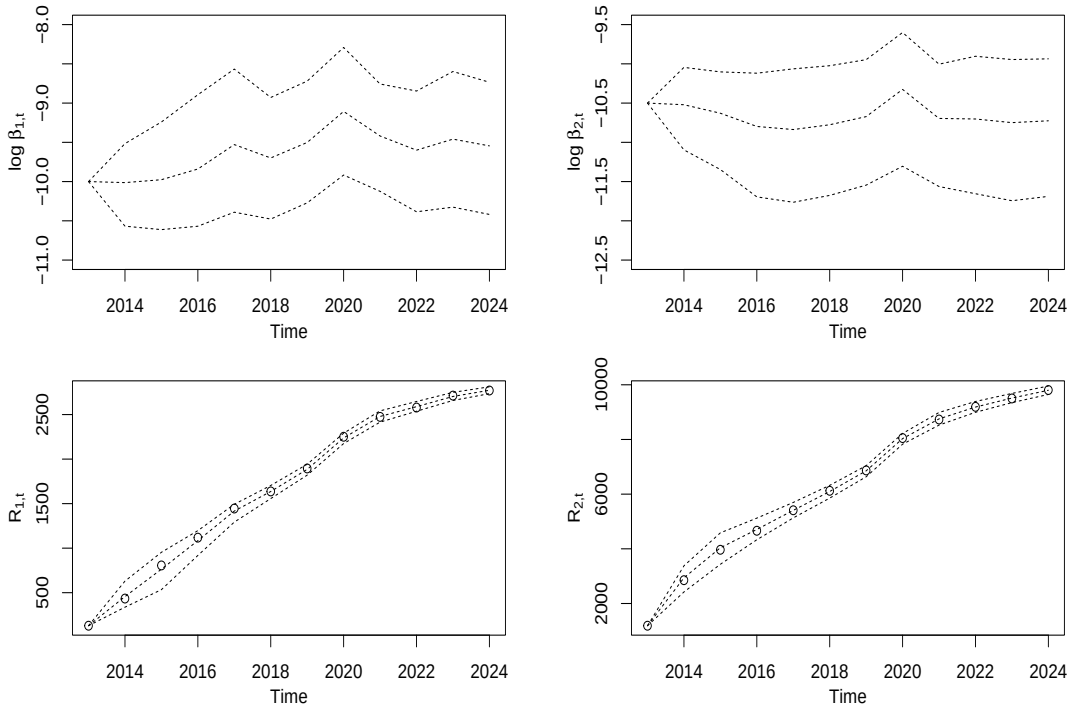

Figure 5: Two-node epidemic example. Marginal filtering means and 95% credible intervals for $\log \beta_{1,t}$ and $\log \beta_{2,t}$ (top panel), and removal prevalences $R_{1,t}$ and $R_{2,t}$ (bottom panel) using the output of NEnKF. Observations are shown as circles.

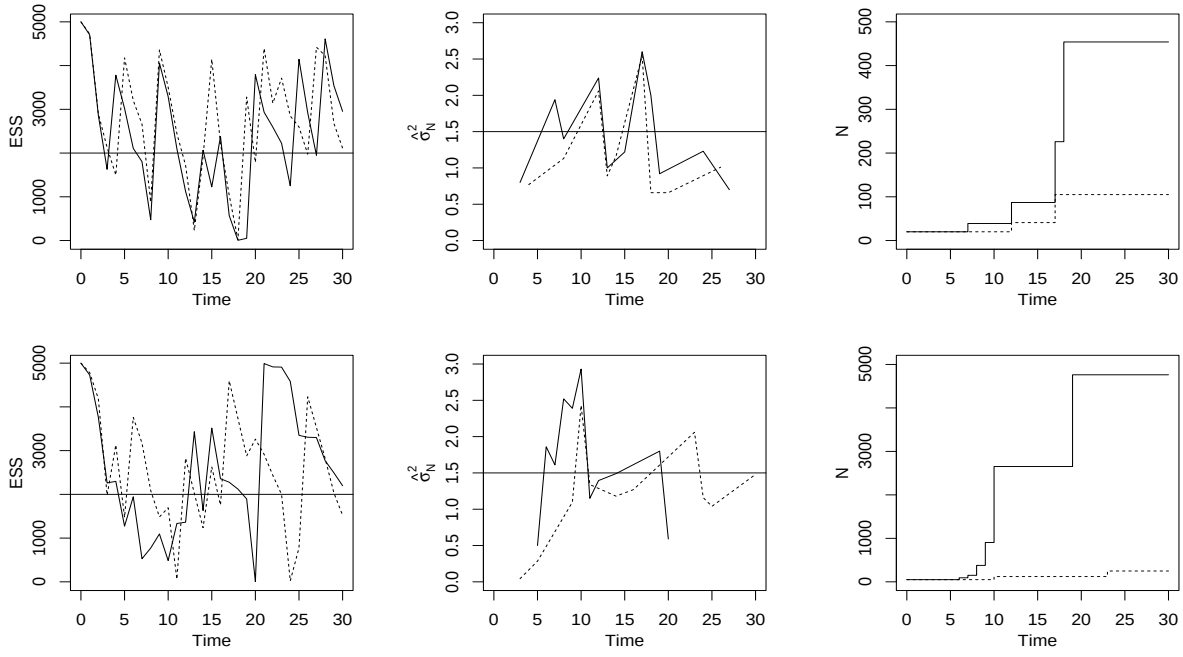

Figure 6: Lorenz 96 example. Effective sample size (ESS) against time (left), $\hat{\sigma}_N^2$ against time and number of state particles / ensemble members N against time. Horizontal lines indicate the thresholds at which resampling and increasing N take place. All results are based on a single typical run of SMC^2 (solid lines) and NEnKF (dashed lines) using data set $\mathcal{D}_1$ (top panel) and data set $\mathcal{D}_2$ (bottom panel).

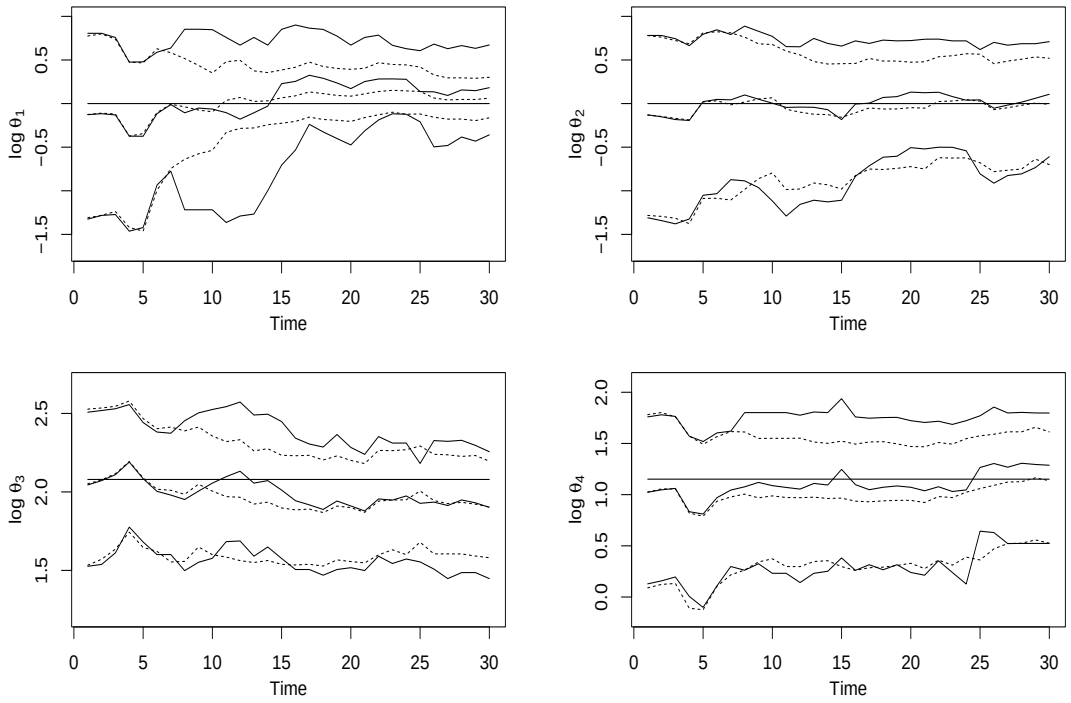

Figure 7: Lorenz 96 example. Marginal parameter filtering means and 95% credible intervals under SMC^2 (solid lines) and NEnKF (dashed lines). For reference, ground truth parameter values are displayed as horizontal lines.